2280 1218

ADA 210767

RD&E CENTER

Technical Report

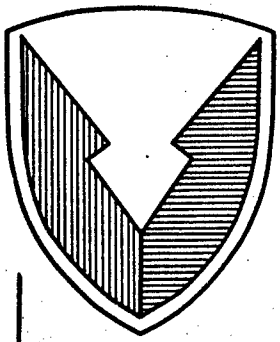

No. 13444

A SURVIVABLE TACTICAL TRUCK RADIATOR

A CONCEPTUAL AND FEASIBILITY STUDY

DAAE07-88-C-R066

JUNE 1989

By T.S. Ravigururajan and M.R. Beltran
Beltran, Inc.
1133 E. 35th Street
Brooklyn, NY 11210

APPROVED FOR PUBLIC RELEASE:
DISTRIBUTION IS UNLIMITED

20031211092

U.S. ARMY TANK-AUTOMOTIVE COMMAND
RESEARCH, DEVELOPMENT & ENGINEERING CENTER
Warren, Michigan 48397-5000

NOTICES

This report is not to be construed as an official Department of the Army position.

Mention of any trade names or manufacturers in this report shall not be construed as an official endoresement or approval of such products or companies by the U.S. Government.

Destroy this report when it is no longer needed. Do not return it to the originator.

REPORT DOCUMENTATION PAGE

Form Approved OMB No. 0704-0188

1a. REPORT SECURITY CLASSIFICATION Unclassified	1b. RESTRICTIVE MARKINGS
2a. SECURITY CLASSIFICATION AUTHORITY	3. DISTRIBUTION/AVAILABILITY OF REPORT Approved for public release: Distribution is unlimited
2b. DECLASSIFICATION/DOWNGRADING SCHEDULE	
4. PERFORMING ORGANIZATION REPORT NUMBER(S)	5. MONITORING ORGANIZATION REPORT NUMBER(S) 13444
6a. NAME OF PERFORMING ORGANIZATION Beltran, Inc. — 6b. OFFICE SYMBOL (If applicable)	7a. NAME OF MONITORING ORGANIZATION U.S. Army Tank - Automotive Command
6c. ADDRESS (City, State, and ZIP Code) 1133 E. 35th Street Brooklyn, NY 11210	7b. ADDRESS (City, State, and ZIP Code) Warren, MI 48397-5000
8a. NAME OF FUNDING/SPONSORING ORGANIZATION — 8b. OFFICE SYMBOL (If applicable)	9. PROCUREMENT INSTRUMENT IDENTIFICATION NUMBER DAAE07-88-C-R066
8c. ADDRESS (City, State, and ZIP Code)	10. SOURCE OF FUNDING NUMBERS PROGRAM ELEMENT NO. — PROJECT NO. — TASK NO. — WORK UNIT ACCESSION NO.

11. TITLE (Include Security Classification)
A Survivable Tactical Truck Radiator - A Conceptual and Feasibility Study (u)

12. PERSONAL AUTHOR(S)
Ravigururajan, T.S. and Beltran, M.R.

13a. TYPE OF REPORT	13b. TIME COVERED	14. DATE OF REPORT (Year, Month, Day)	15. PAGE COUNT
Final	FROM 88 8/9 TO 89 5/9	89 June 30	84

16. SUPPLEMENTARY NOTATION

17. COSATI CODES			18. SUBJECT TERMS (Continue on reverse if necessary and identify by block number)
FIELD	GROUP	SUB-GROUP	Survivable tactical truck radiator Heat pipes

19. ABSTRACT (Continue on reverse if necessary and identify by block number)

The single most important design factor faced by the cooling systems in tactical trucks is their vulnerability to exploding shells, sniper fire, and other projectiles. This project proposes to use heat pipes in radiators to transfer waste heat from the engine to the surrounding environment. In the phase I concept feasibility study, a computer program was developed to design a small scale heat pipe radiator module. Experimental tests were performed on this maodule to test the validity of the design methodology and to study the vulnerability characteristics of the heat pipe radiator for a wide range of operating parameters such as air velocity, coolant flow rates, and the number of heat pipes damaged. The results showed that a heat pipe radiator will provide the necessary limp home capability for tactical trucks even with 50 % of the heat pipes damaged. Also, when the radiators are operating at less than peak capacity (slower vehicle speeds), the undamaged heat pipes substantially compensated for the damaged heat pipes adding to the reliability of the system. The development and testing of a prototype will be taken up in the Phase II of the program

20. DISTRIBUTION/AVAILABILITY OF ABSTRACT ☒ UNCLASSIFIED/UNLIMITED ☐ SAME AS RPT. ☐ DTIC USERS	21. ABSTRACT SECURITY CLASSIFICATION Unclassified
22a. NAME OF RESPONSIBLE INDIVIDUAL M. L. Goryca	22b. TELEPHONE (Include Area Code) (313) 574-8532 — 22c. OFFICE SYMBOL AMSTA-RGT

DD Form 1473, JUN 86 — Previous editions are obsolete.

TABLE OF CONTENTS

LIST OF ILLUSTRATIONS

LIST OF TABLES

1.0. INTRODUCTION

This final technical report, prepared by Beltran, Inc., for the U.S. Army Tank-Automotive Command (TACOM) under Contract DAAE07-88-C-R066, describes Phase I work in the development of a survivable tactical truck heat pipe radiator. Combat/tactical military vehicles face difficult operating and terrain conditions. These vehicles are normally provided with armor; yet, their protection depends on their operating condition and other tactical criteria. For this purpose, the engine and its supporting systems are enveloped in an armored compartment within the vehicle, with airflow through metallic grilles. The space for the cooling system in the engine compartment is quite restricted.

The single most important design factor faced by the cooling system is its vulnerability to exploding shells, sniper fire and other projectiles. At present, these threats are minimized by providing ballistic grills, or placing the system in an armored envelope.

This project proposes to use heat pipes in radiators to transfer heat from coolant to air (or from other liquids like transmissions and hydraulic oils). If one or more heat pipes are damaged, the remaining pipes can pick up the load. This will increase the reliability of the radiator. This feasibility/conceptual study shows the effectiveness of a heat pipe radiator.

2.0. OBJECTIVE

It is the objective of the Phase I project, by using a model heat pipe network module, to:

- develop a computer model
- design, fabricate, test and evaluate radiator
- deliver a radiator test section to TACOM

3.0. CONCLUSIONS

The analytical and experimental work has shown that these objectives are practical and can be implemented successfully in a prototype radiator. The salient features of the study were as follows:

- The analytical and experimental study proved the correctness of the design methodology and approach to

be adopted in the Phase II work on the prototype heat pipe radiator.

- The effect of air flow rates is to increase the performance drastically before levelling off at very high velocities.
- At high engine RPM, the heat pipe radiator performed at 85% capacity even with 25% damage to the cone.
- At lower engine RPM, the radiator performance was nearly constant, even with 30% damage.
- The pressure drop for this module exhibited the anticipated trend. It increases with air velocity rising more steeply at higher values.
- Even at slopes of 60 degrees, the heat exchanger was able to perform at greater than 80% capacity.
- The heat pipe radiator module is more efficient by 25% than similar conventional radiator.
- A considerable size and weight reduction, by up to 25%, may be anticipated in a heat pipe radiator.

4.0. RECOMMENDATIONS

Having proved the concept, the next logical step is to develop a prototype radiator for a typical engine for the M939A2 vehicle. This should be done in several stages.

- The radiator should be designed for thermal performance according to specification AMCP 706-361, taking into account the operating and ambient conditions and other severity conditions, and several factors such as:

  - long term - storage
  - mechanical design (shock, vibration, etc.)
  - terrain conditions

  A comprehensive computer program should be developed that will design the best elemental heat pipe and the overall radiator design. The thermal design may take into account the freezing of heat pipes, the overload factor, design of coolant pump and fan.

- With the thermal design in place, the configuration design should be done to adapt to existing

radiators. This will include the overall dimensional constraints, mounting techniques and maintenance criteria.

- The fabrication and the experimentation of the radiator should be carried out in a laboratory environment, followed by an actual demonstration on a truck.

- A cost study for the heat pipe radiator production and a comparative analysis with the existing conventional radiator would be necessary as part of the prototype of a survivable heat pipe radiator.

5.0. DISCUSSION

5.1. Background

Cooling systems in I.C. engines play a very important role in rejecting waste heat (Figure 5-1). However, the tatical/conmbat vehicles used by the Armed Forces are handicapped by the vulnerability of the radiators[1-6]. It is the goal of the study to use heat pipes for the radiators that will eliminate or greatly reduce the radiator vulnerability.

The heat pipe is being increasingly studied for a wide variety of applications involving different heat transfer processes. These applications vary from the cooling of electronic chips to space power generation [7-10].

The heat pipe's wide potential may be attributed to its unique characteristics.

- Good thermal response time. Vapor in the heat pipe travels at nearly the speed of sound. For example, if a heat pipe is dipped in 80°C water, the other end of the heat pipe will reach 80°C almost immediately. This characteristic is especially important for the proposed design.

- Extremely high thermal conductivity. The heat pipe has an effective thermal conductivity which is 200 times that of copper. This means that for the same size and heat transfer rate, the temperature difference required to maintain that rate would be 200 times greater for the copper bar than the heat pipe. In terms of the proposed design, this means that a 200 times greater heat transfer rate can be obtained with a heat pipe

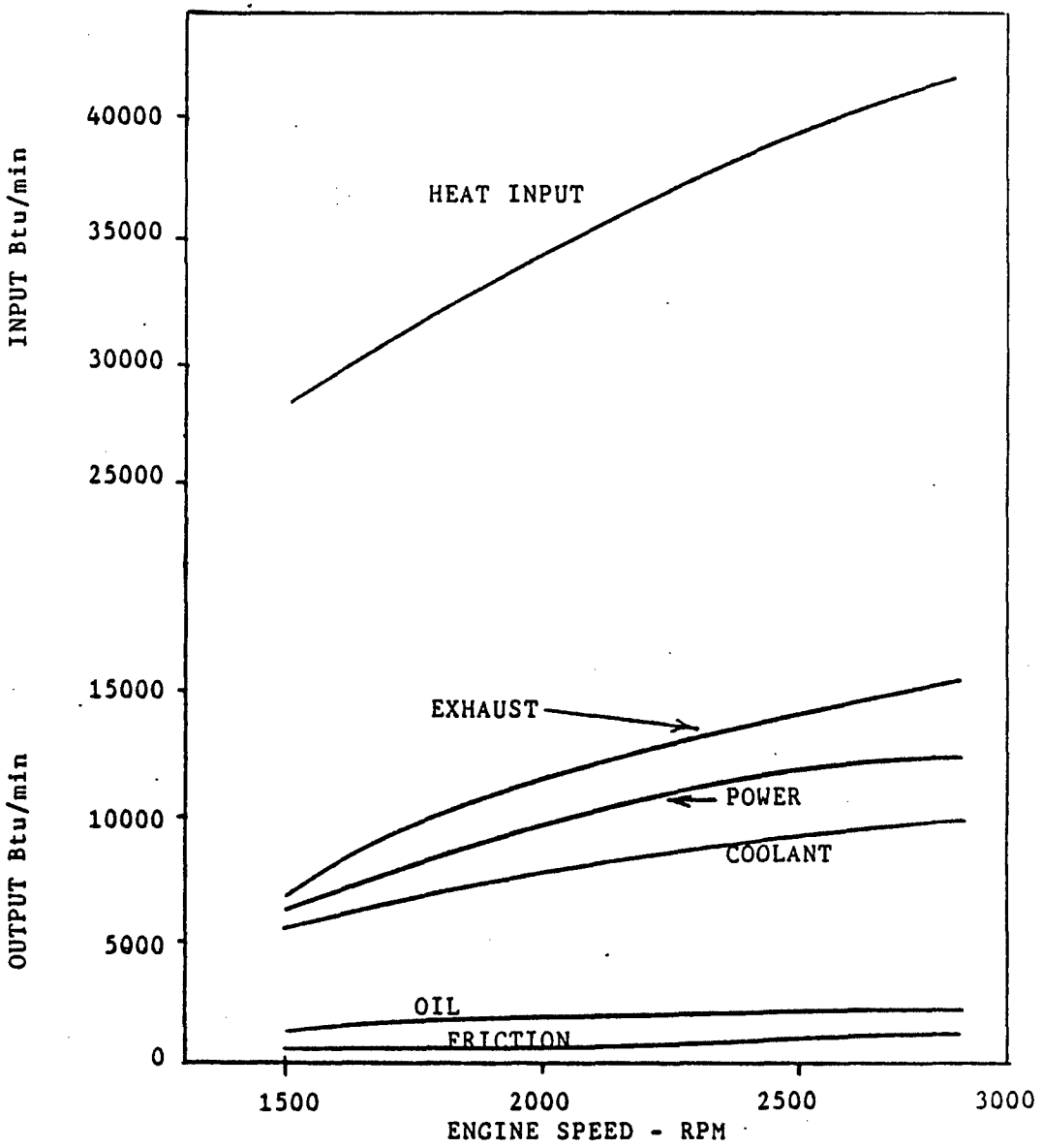

FIG. 1 THERMAL CHARACTERISTICS OF A TYPICAL ENGINE

Figure 5-1. Thermal Characteristics of a Typical Engine

than with the same size copper rod for the same temperature difference between the ends.

- Temperature uniformity. Uniform temperatures of each part in the heat pipe can be obtained throughout its length. What this means for our design is that a temperature gradient is produced along the length of the heat pipe, but that at each section, the temperature is constant at all points around the heat pipe.

- Flexibility in design. The heat pipe allows heat transfer between the two ends, and the actual configuration used does not restrict the ability to accomplish the transfer. Thus the materials used to construct the casing may be flexible and easily conform to the particular component or part of vessel. The working fluid inside the heat pipe becomes the one thing that must be selected for the operating range of temperatures involved.

- Heat pipes are maintenance-free; they function without being driven electrically or mechanically. Thermal and chemical stability on the inside is adequate. Perfect operating conditions are maintained over long periods of time without maintenance. This is an especially desirable feature for ensuring continued use of the device by personnel.

- Heat pipes are lightweight and compact. While this advantage is not important in many engineering applications, it is especially important when interfacing a heat pipe to an existing equipment. Even if heat pipes had all the superior characteristics listed above, if this one were lacking, the system design using heat pipes would not be feasible.

- Heat pipes are more cost effective than most other heat transfer devices. They are reasonably simple to manufacture, which results in cost savings during initial implementation. Heat pipes are reliable, require virtually no preventive or corrective maintenance during their operating lifetime.

An important design consideration in the thermal design of a heat exchanger is the determination of its heat transfer rate and the heat rejected from an engine can be estimated approximately[11-15]. In a heat pipe heat exchanger, the pipes may be horizontal, or vertical with the evaporator sections below the condensers. The angle of the heat pipes may be adjusted "in situ" as a means of controlling the heat

transport. This is a useful feature that can be employed in radiator applications.

Although the heat pipe exchanger has only been in mass production for approximately a decade, their development and use indicates a very wide range of applications in industry and commercial and municipal buildings. Their use in liquid-air heat exchangers, and in particular, radiators, will increase the heat transfer ability noticeably. In conventional radiators, the mechanism of heat transfer is single phase convection. Replacing plain tubes with heat pipe will introduce boiling and condensation. The increase in heat transfer coefficient due to two-phase flow is manifold, resulting in a highly efficient and smaller radiator.

5.2. Analysis and Evaluation

Heat pipes, due to their efficiency and simplicity of operation, are finding increasing use in industrial applications, including space and electronic equipment. Yet the design of a heat pipe is more complex than other heat transfer equipment. This is because of the many processes that take place simultaneously in a heat pipe. These include liquid and gas phase flows, condensation and evaporation (with suction or blowing), mass transfer, interfacial energy transfer, heat gain or loss through conduction, convection and radiation, among other processes. In most applications and designs of heat pipes, all the processes and variables are interdependent, which adds to the intricacy of the problem. In spite of the numerous variables involved, detailed knowledge on each of these processes has simplified the design of heat pipes.

5.2.1. Governing Equation.

The main regions of a heat pipe are shown in Figure. 5-2. The heat is absorbed in the evaporator section wherein the working liquid boils at the wick surface. The vapor then moves to the condenser section and condenses rejecting heat. This heat can be removed from the heat pipe through an appropriate technique. The condensate is returned to the evaporator section through the capillary pumping due to the wick pore and the surface energy of the liquid. The central section is the adiabatic section where a pump may be installed to import additional pumping power.

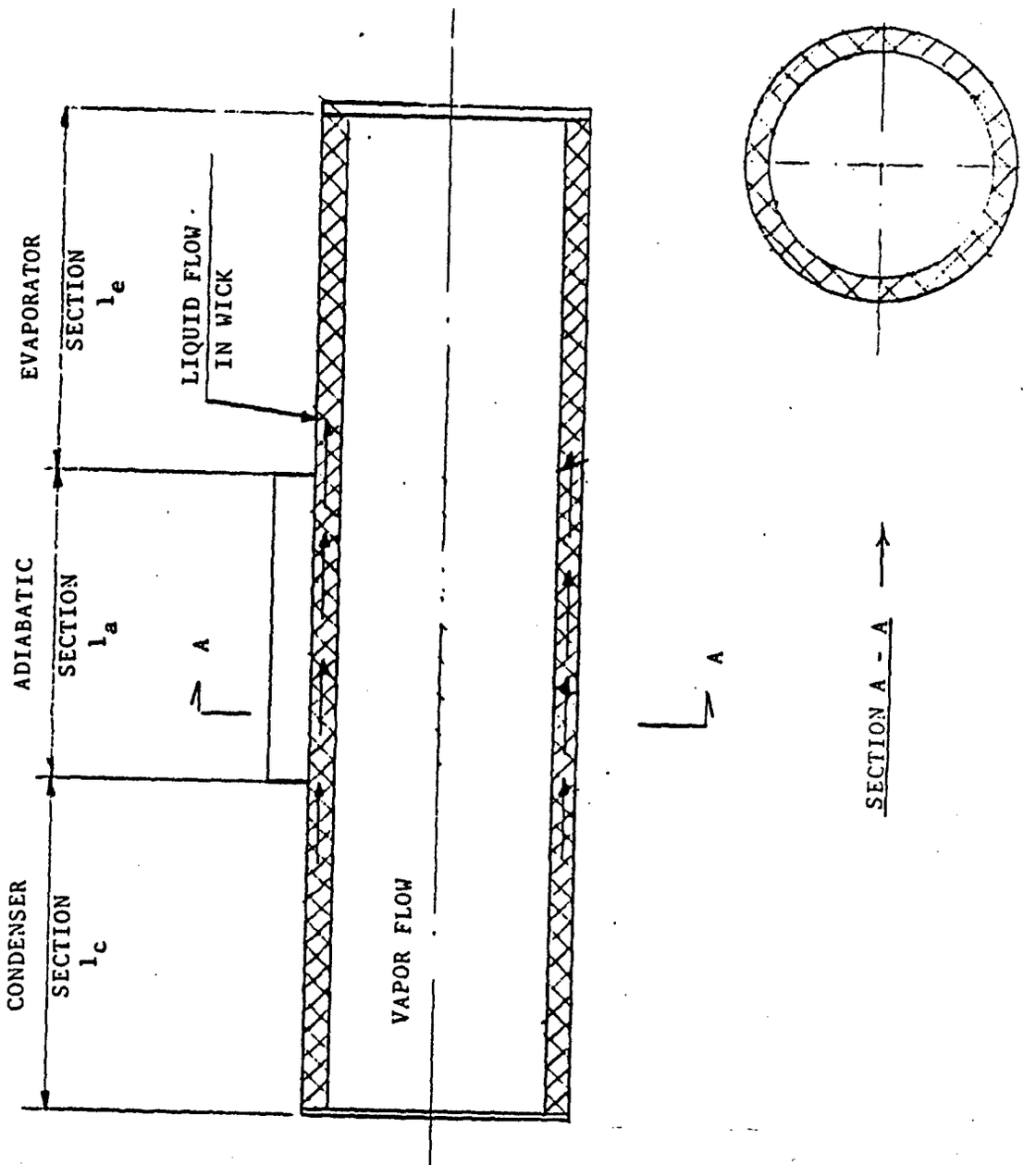

Figure 5-2. A Schematic Diagram of a Typical Heat Pipe

The driving force for the working fluid in the heat pipe is provided by the capillary force while pressure loss is incurred due to viscous drop in liquid and vapor, inertial loss due to the vapor flow. Gravitational force can act for or against the liquid, depending on the flow direction.

The governing equation can then be expressed as

$$\Delta P_l + \Delta P_v + \Delta P_g \leq \Delta p_c \qquad (1)$$

where

DP_l = liquid viscous drop

ΔP_v = viscous and inertial vapor pressure loss

ΔP_g = gravitational pressure drop

Δp_c = capillary force

In physical terms, the capillary limit determines the flow rate, and hence, the capacity of the heat pipe, by balancing the various pressure loss components.

Substituting the expressions for the pressure drop losses in liquid and vapor, both viscous and inertial, and the driving force of capillary action (also known as wicking action), the governing equation for the heat pipe can be expressed as:

$$Q\mu_l/\lambda\rho_l A_{wl} + (4Q/\lambda\rho_v A_v)(8\mu_v/r_v^2[(l_e + l_c)/2 + l_a]$$
$$+ (Q/\lambda\rho_v A_v)^2 l_v - 2\sigma_c/r_c + \rho_l g l = 0$$

The heat load for the heat pipe can be found from the quadratic equation

$$\alpha Q^2 + \beta Q + \gamma = 0 \qquad (2)$$

where

$$\alpha = (1/\lambda A_v)^2 \, 1/\rho_v \qquad (a)$$

$$\beta = \mu_l/\lambda\rho A_w K\left[[(l_e + l_c)/2 + l_a]\right]$$
$$+ 8\mu r/\lambda\rho\pi r_v^4 \, [(l_e + l_c)/2 + l_a] \qquad (b)$$

and

$$\gamma = -[2\sigma_c - \rho_l g l] \qquad (c)$$

While the capillary pumping determines the priming capacity and functionality of a wicked heat pipe, several other constraints can reduce or hinder efficient operation of a heat pipe and in certain instances can lead to total breakdown. Because of this possibility, in heat pipe design and analysis these associated constraints are always taken into consideration. The various constraints are discussed briefly in the following section.

5.2.2. Constraint factors.

In addition to capillary force limitation, several other factors such as sonic limitation, entrainment condition, boiling constraint and condenser heat removal capability impose severe restrictions on the operation of a heat pipe. The severity of these limitations is determined by several variables such as the working fluid, operating temperature, the wick structure, and the length of the heat pipe, among others[16-21].

5.2.2.1. Sonic limitation

The sonic limitations in heat pipes are similar to the ones encountered in a converging-diverging nozzle. The constant mass of vapor changes its velocity as a function of the cross-sectional area. In heat pipes, the velocity is a function not of area of vapor flow, which is constant, but of the mass flow rate, which changes due to "suction" and "blowing" phenomena associated with the condenser and evaporator regions. The increase in vapor velocity reaches choking condition as the evaporator exit pressure is reduced. Any heat transport beyond the point is not feasible.

5.2.2.2. Entrainment Limitation

In a heat pipe, the vapor flows from the evaporator to the condenser and the liquid is returned by the wick structure. At the interface, the vapor exerts a shear force on the liquid in the wick, which depends on the vapor properties and velocity, and its action entrains droplets of liquid and transports them to the condenser end. Entrainment limits the heat pipe operation and performance, and hence, cannot be exceeded.

5.2.2.3. Boiling Limitation

The limitation of boiling, or the burnout condition, is usually higher than other limits. However, the length of the evaporator depends on the boiling capabilities of the wick structure and, as such, boiling characteristics of wick surfaces are needed for optimum design of heat pipes.

5.2.2.4. Heat Transfer Constraint

The heat transported by the heat pipe depends directly on the heat lost to the sink. That is, the transfer of thermal energy from the condenser region to the surrounding environment stabilizes the working fluid circulation in the equipment, thereby establishing another important design criterion. For terrestrial applications, the control of the condenser region is somewhat easier, since several parameters such as the length of the condenser, the temperature, and the mass flow rate of the coolant can be varied for satisfactory operation. The designs of such subsystems are well known and have been described in detail in several references[22-26].

The overall radiator capacity depends on the heat transferred from 1) engine coolant to the heat pipes, and 2) heat pipes to the air flow. These two limits are in turn set by the heat exchanger design, including the tube spacing and arrangement, fluid flow rate and the available surface area. The principles and the correlations governing the flow across tube banks are outlined below.

The tube rows of a bank are either staggered or aligned in the direction of the cross flow velocity. The average heat transfer coefficient for the entire tube bundle for airflow is obtained from a correlation suggested by Zhukasskas[27]. Reynolds number is given as

$$RE_{D,max} = \rho V_{max} D/\mu \qquad (3)$$

with V_{max} being the maximum velocity occurring in the tube bank. All properties are evaluated at the mean film temperature. The values of C_1 and in Eq. (3) depend upon the transverse pitch S_t, the longitudinal pitch S_L and the outer diameter D of the tubes.

For the aligned arrangement, V_{max} occurs at the plane A and is calculated from the expression

$$V_{max} = S_T/(S_T - D)\ V_\alpha \qquad (4)$$

For the staggered arrangement V_{max} may occur either at the plane A or the inclined plane B. For plane A, the value of V_{max} is again given by Eq. (4), while for plane B

$$V_{max} = S_T/[(4\ S_L^2 + S_T^2)^{1/2} - 2D]\ V_\alpha \qquad (5)$$

Equation (5) is also used for fluids (other than air) having Pr> 0.7 by multiplying by the factor 1.13 $Pr^{1/3}$. Thus we have

$$\overline{Nu}_D = 1.13\ C_1\ Re_D^{m,max}\ Pr^{1/3} \qquad (6)$$

If the number of rows is less than 10, then the Nusselt numbers given by Eq. (6) is multiplied by a correction factor C_2.

A correlation for the pressure drop across banks of tubes has also been given by Zhukauskas in the following form:

$$\Delta P = 4\ f\ N\ X\ (\rho V^2_{max})/2 \qquad (7)$$

The heat transfer coefficient can now be easily determined and the total heat transfer is given by

$$Q = UA\Delta T_{LMTD}$$

where

U = the overall heat transfer coefficient.
A = surface area
ΔT_{LMTD} = log mean temperature difference.

It is clear from the expression that the temperature, flow rate and the surface area can be controlled. But even this control is limited, since the temperature of the condenser is a function of the working fluid properties and the condenser geometry is dictated by size and weight restrictions. As a result, the radiation constraint plays a very important role in the design of heat pipes.

The various constraints discussed above along with the requirements decide the ultimate design of a heat pipe.

5.3. Phase I Work

5.3.1. Conceptual Radiator Design. Developing a computer program to design the "Model" heat pipe heat exchanger was the initial step of the project. The design of a liquid-air heat pipe heat exchanger consists of three separate stages, namely, the elemental heat pipe, the heat pipe to air exchanger, and the liquid chamber which transfers the heat

from the coolant to the heat pipe. The heat transfer capacity of each segment should be more than the specified heat duty at required condition. This ultimate design can usually be accomplished through several iterations. A flow chart explaining the methodology of the heat pipe heat exchanger design is outlined below.

The problem involves good engineering judgments, numerous variables and sometimes may involve several iterations before arriving at an adequate design. The overall design methodology involved in the sizing of a heat pipe heat exchanger is shown in Figure 5-3 The outside fluid stream inlet temperatures, pressure drops and possibly exchanger size limitations are specified as well as either the required outlet temperatures, heat duty or the effectiveness of the heat exchanger are specified. An effective method is to couple the specified heat transfer and pressure drop information to obtain an approximate size, and iterate on it, as is done for conventional heat exchangers.

Mathematically, the design should satisfy the broad condition:

$$Q_{design} = Q_{HP} = U_a A_a LMTD_a = U_w A_w LMTD_w \qquad (8)$$

Based on the heat duty and the length constraints of the radiator, the heat pipe is designed for the optimum diameter that will satisfy the governing equation and the accompanying constraints outlined previously (Section I in Figure 5-3). Once the number and the geometry of the heat pipes are known, the design of the air-heat-pipe heat exchanger can be designed (Section II). A similar design solution is necessary to satisfactorily transfer heat from the engine coolant to the heat pipes (Section III).

The most important factor is, of course, that the heat exchanger must meet the design requirements. That is, it must transfer the desired energy to the air stream within the allowable pressure drops. Another factor is that the exchanger must withstand the service conditions of the radiator. This includes the mechanical stresses of installation, startup, shutdown, normal operation, emergencies, and maintenance, and the thermal stresses induced by the temperature differences. The exchanger should also resist fouling;however, there is not much a designer can do with confidence in this regard except to keep the velocities as high as pressure drop and vibration limits permit.

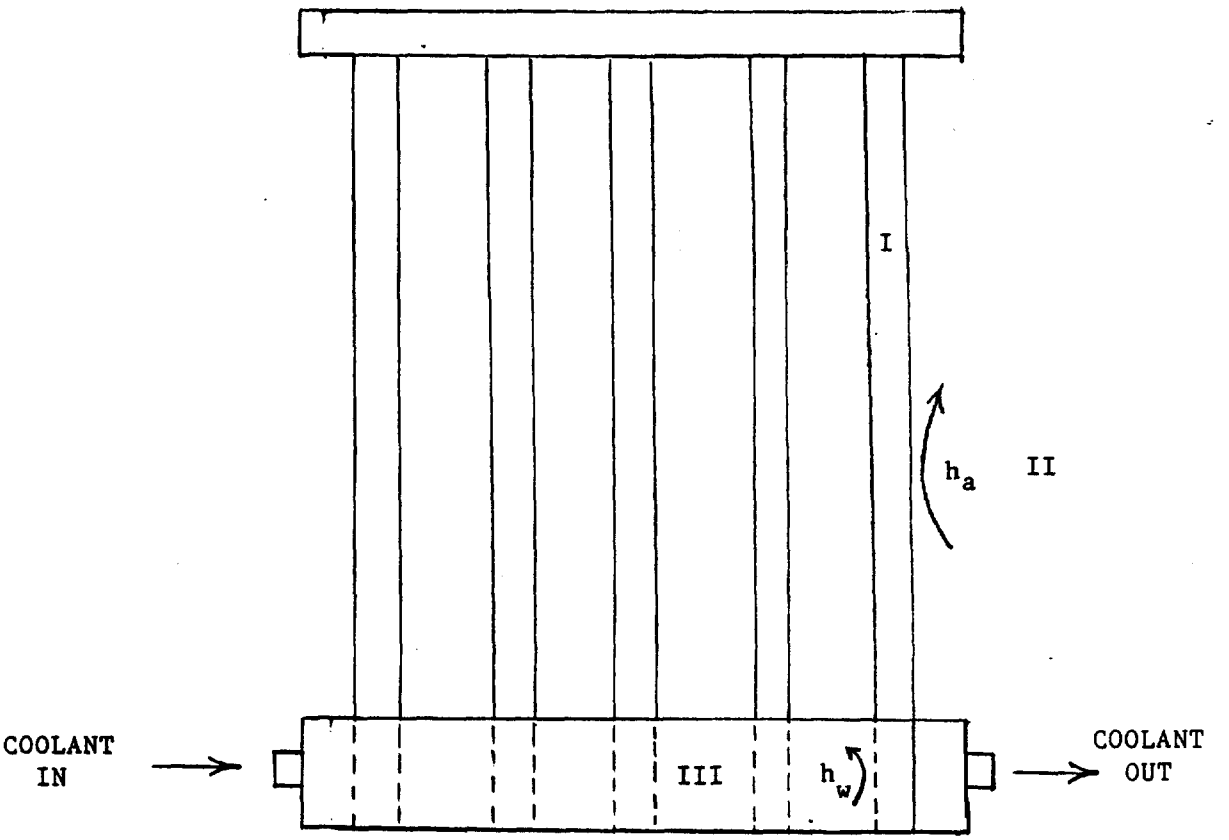

SEGMENT I - Heat Pipe Design SEGMENT II - Heat Pipe - Air Exchanger Design

SEGMENT III - Heat Pipe - Coolant Exchanger Design

Figure 5-3. Design Methodology of a Heat Pipe Radiator

Maintenance, cost, and other installation conditions must also be taken into account when the final design and fabrication is taken up.

The logical structure of the heat exchanger design procedure is shown in Figure 5-4. The procedure essentially consists of the three design subdivisions structured to suit a computer.

First, the design of the heat pipe is carried out. The working fluid, operating temperature, heat pipe diameter and wick structures were selected as representative of current practice and the operating conditions of the radiator. The length of the condenser was such as to make full use of the capillary limitation and the rejection constraint. The solution by iteration of the following equations yields the maximum condenser length based on the pressure drop along the heat pipe circuit.

$$(8\dot{m}\mu_v/\rho\pi r^4 + \mu_l v_l/K)\ (l_e/2 + l_a) - \rho_v v_v^2 + \rho_l g = 0$$

$$Q = h_a A_a \Delta T_{LMTD} \qquad (9)$$

with

$$Q = \rho_l A_l V_l \lambda = \rho_v A_v V_v \lambda \qquad (10)$$

The resulting condenser length will provide the maximum power at full capillary pumping. Further increase in length will add significantly to the condenser capacity to reject heat, subject, of course, to constraints discussed previously. The length of the evaporator and the condenser sections of the heat pipe are determined by trial and error to match its pumping capacity. The diameter of the heat pipe is changed repeatedly to obtain the minimum number of pipes required for the designed load.

Once the heat pipe design is established, the program solves the design of the heat pipe - air exchanger (Figure 5-5), including the transverse and longitudinal pitch, number of rows and columns, and the heat transfer coefficient. In this segment, the problem specifications and a preliminary estimate of the exchanger configurations are used as input data; it computes a number of internal geometry parameters - surface, flow areas, etc., that are required as further input into the heat transfer correlations and the pressure drop correlations. The exchanger configuration assumed is tested for its ability to effect the required energy transfer from the heat pipes to the outside air stream subject to the pressure drop limitations. This is

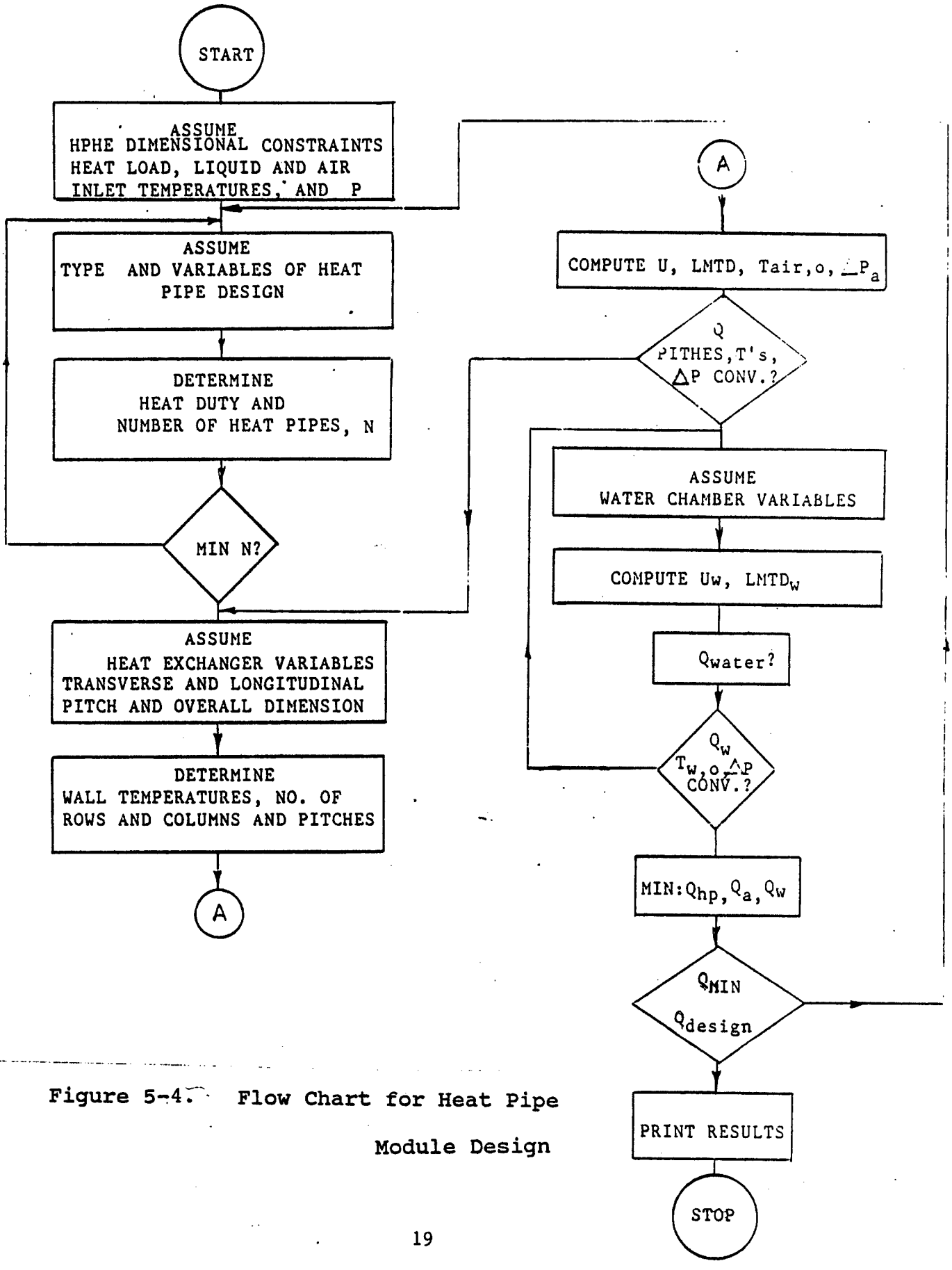

Figure 5-4. Flow Chart for Heat Pipe Module Design

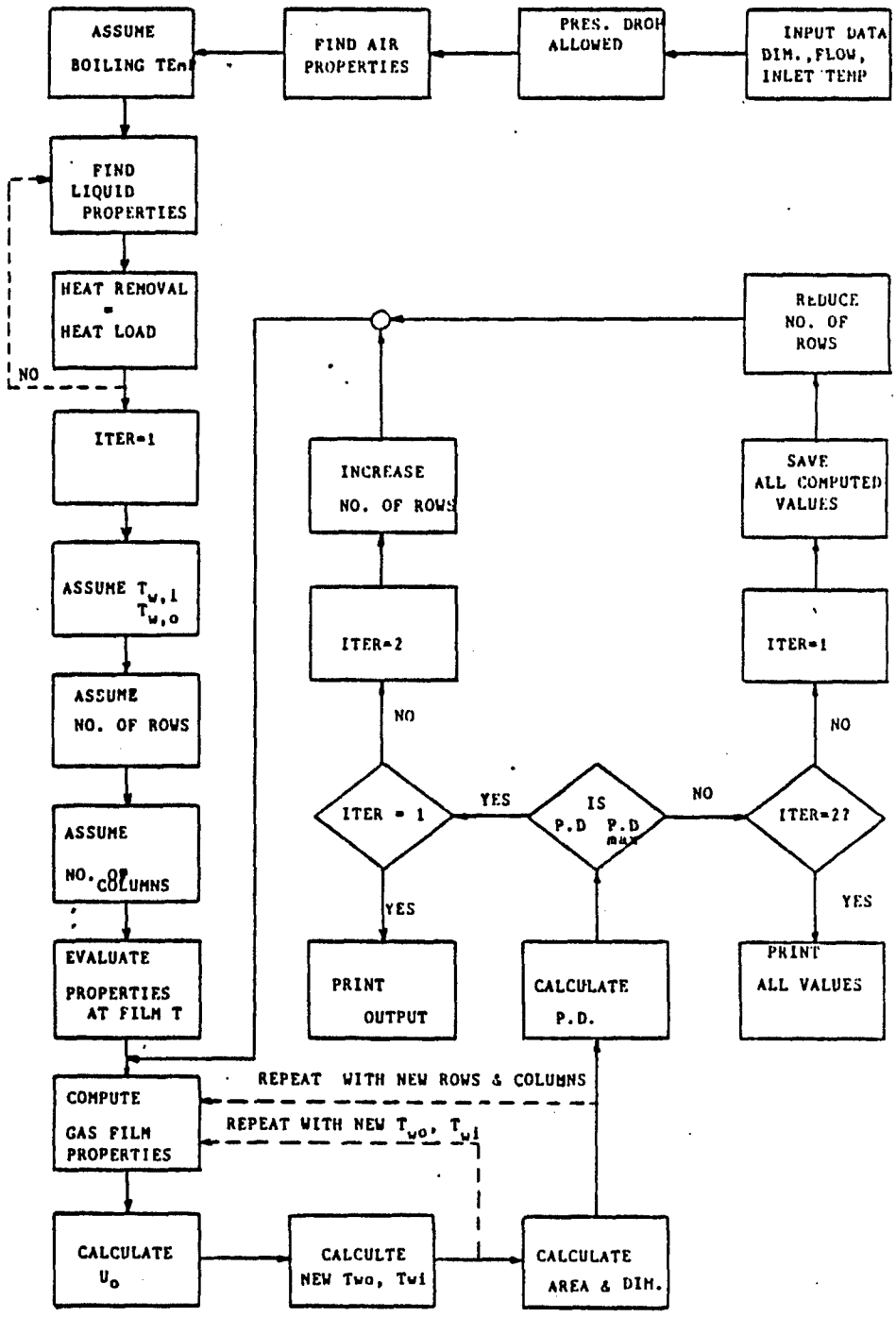

Figure 5-5. Flow Chart for Air-Heat Pipe Exchanger Design

accomplished by using appropriate correlations - heat transfer and pressure drop - are calculated for the stream in the configuration specified. A careful analysis is required in generating this segment of the program because it is in this section that all of the necessary correlations for heat transfer and pressure drop are put in quantitative form by the heat exchanger designer. These correlations usually come from theoretical and experimental analyses.

This step sets the performance limits of the heat exchanger. Parameters are varied to remove those limitations without adversely affecting those operational characteristics of the exchanger that are satisfactory. The configuration, specifically, the transverse and longitudinal pitch, the rows and columns, and the air outlet temperature are varied in obtaining the minimum area required for the energy transfer. For example, if the heat exchanger is limited by the amount of heat that it can transfer, the program will try either to increase the heat transfer coefficient or to increase the area of the heat exchanger. To increase the coefficient, one can increase the number of rows, thereby increasing the air velocity. This also increases the area due to the higher number of pipes. Other parameters that can be varied include heat pipe arrangement, pressure drop, air outlet temperatures, heat pipe diameter, and possibly fin dimensions.

If the exchanger is limited by pressure drop, the program changes the number of rows of pipes, and hence, the air velocity.. The design parameters obtained at the convergence of this stage of program will yield the area, in other words, the number of heat pipes, necessary for the heat transfer to air. If the surface area is not sufficient to transfer the rated thermal load, the heat pipe diameter is changed. Consequently, the heat pipe design and the exchanger is re-rated.

The third stage of the program involves the design of water chamber which is very similar to the rating problem of air-heat pipe exchanger. The water flow rate and the water or the coolant outlet temperature is determined through iteration so as to be able to transfer the specified heat load.

The solution from the three segments are iterated several times until the heat transferred from the coolant to heat pipe, heat pipe capacity, and the heat pipe to air heat transfer converge to the required conditions.

5.3.2. Experimental Apparatus. The investigation was carried out in an air flow facility in our laboratory. A

photograph of the experimental setup is shown in Figure 56. A description of the facility may be divided into two categories, the air side and the coolant side.

The airflow facility used is an open circuit blowing-type wind tunnel using a centrifugal fan driven by a 5-horsepower motor. The fan has a maximum rated capacity of 3500 cfm and a head of 6 inches of water. Since the motor is a constant speed-type, the airflow rate is controlled by a combination of dampers and inlet guide vanes. Figure 5-7 shows the general configuration of the tunnel.

The downstream end of the test section consists of instrumentation modules, between which the heat exchanger core is installed. These instrumentation sections are designed to accept measuring instrument probes on the top and one side.

As shown in the schematic in Figure 5-8, the coolant loop is a closed system for circulating hot coolant through the coolant chamber. Coolant from the insulated storage tank is pumped through the core coolant chamber by a centrifugal pump.

The piping consists of 1-inch galvanized steel piping insulated by 1- to 1.5-inch fiberglass insulation. A 10-kW electrical heater is provided in the tank to maintain coolant at the desired temperature while the coolant passes through four tubes. The hot coolant, approximately at 180^{o}F, passes through a flow control valve and enters the tank of the heat pipe heat exchanger through a variable area flowmeter (rotameter). The cooled water leaves the heat exchanger and returns to the storage tank.

The heat pipe heat exchanger consists of a coolant chamber connected by heat pipes to the frame. The typical test core is shown in Figure 5-9. Aluminum flanges were attached to the frame with screws so that the core assembly could be mounted between the instrumentation modules.

The data measured included inlet and exit air temperatures, inlet air velocity, upstream and downstream static pressure, inlet and exit coolant temperatures and coolant flow rate.

5.3.2.1. Air Side. Inlet air temperatures were measured using two copper-constant thermocouples. These two thermocouples were traversed horizontally across the test section, 6 inches vertically apart. The thermocouples were mounted in stainless steel tubing attached to two traversing actuators fixed to the inlet side module.

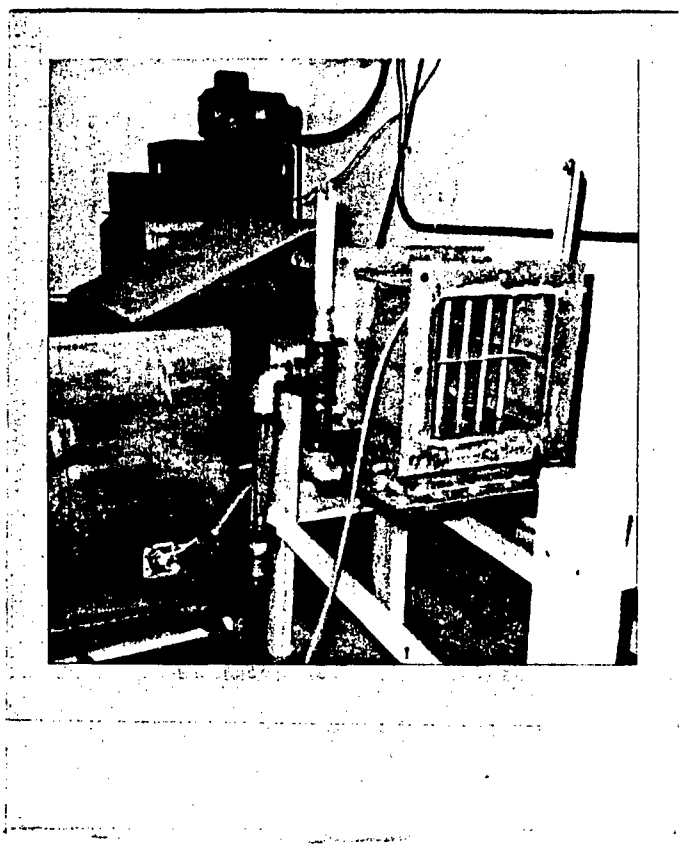

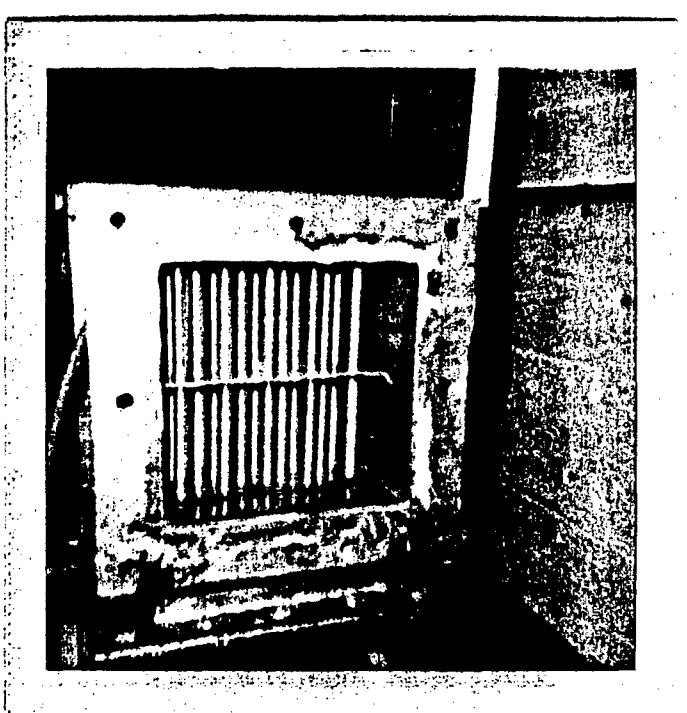

Figure 5-6: Photos of the Experimental Rig and the Model Heat Pipe Heat Exchanger

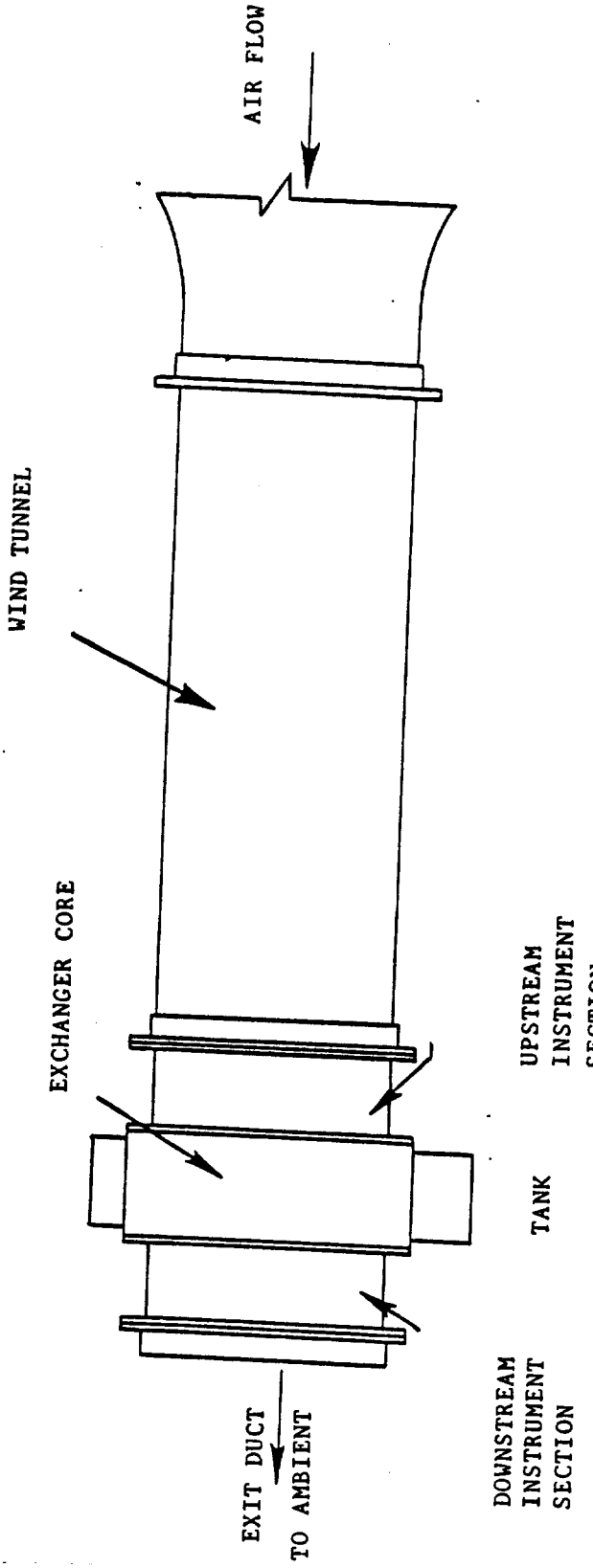

FIG. 5 SKETCH OF AIR FLOW CHANNEL

Figure 5-7. Sketch of Air Flow Channel

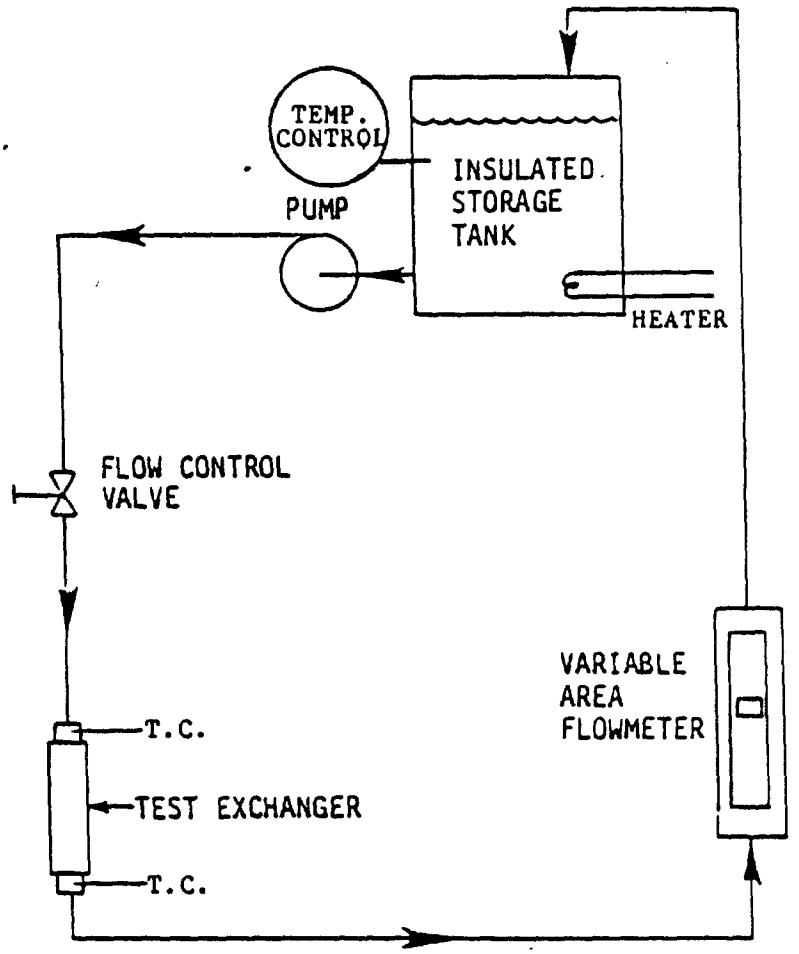

Figure 5-8. Coolant Flow Circuit

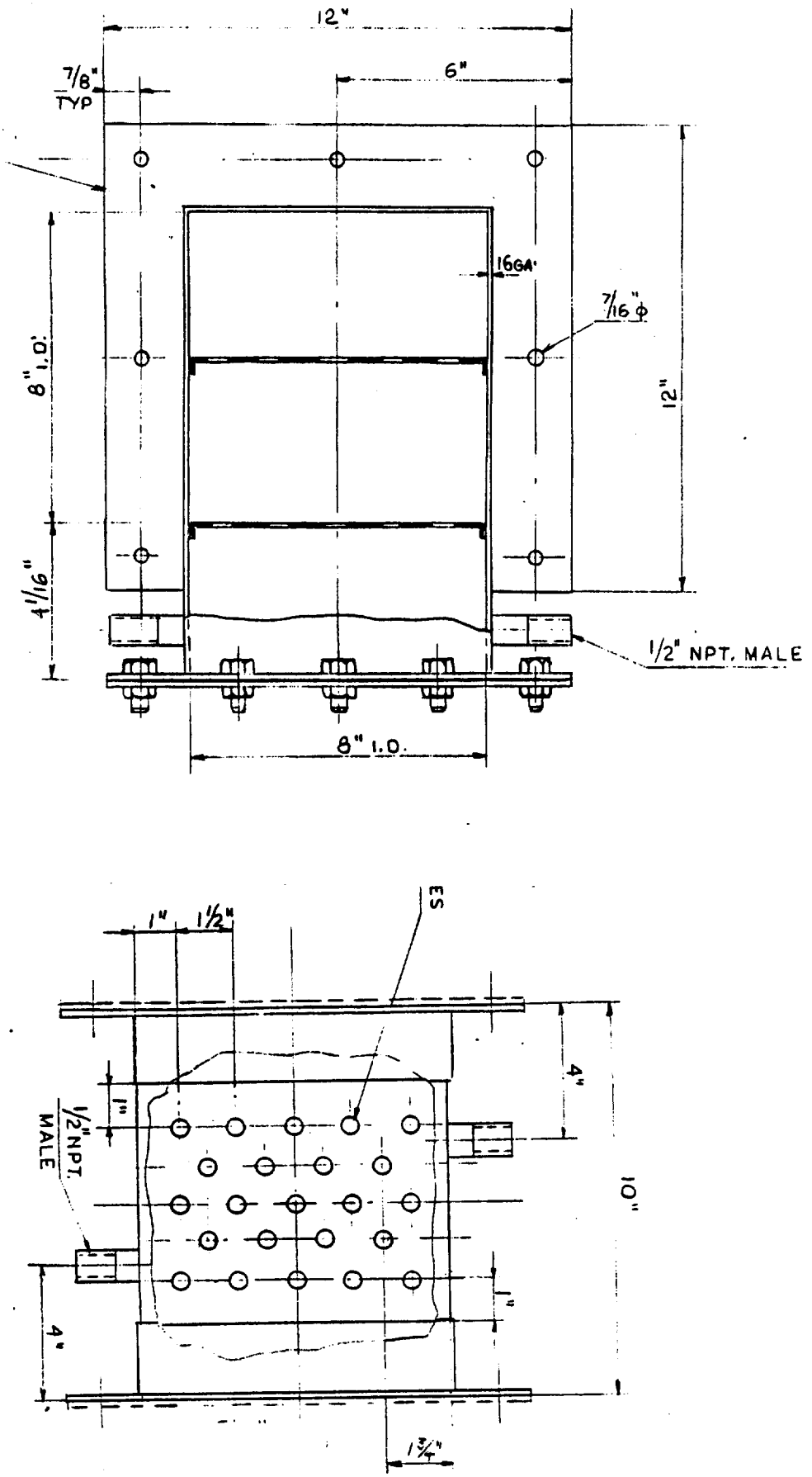

Figure 5-9. Drawing of the Model Heat Pipe Heat Exchanger

Exit air temperature measurements were made using similar thermocouples. At the exit side, there is a wide variation of air temperature from the top to the bottom, and it is necessary to sense the temperature distribution. This was accomplished through averaging across the channel.

Pressure measurements were taken at the two instrumentation modules and at the instrument port upstream of the grid location. At the upstream instrumentation module and at the point ahead of the grid, the total pressure and the static pressure were measured using two pitot static probes. These probes were mounted so that they could be traversed to the center of the test section when the measurement was to be made. The inlet air velocity was calculated using the total and static pressures measured at these locations. Since the velocity was not uniform immediately downstream of the grid, the pressure measurement at the inlet was used for purposes of mass flow measurements.

A static pressure probe was used to measure the outlet static pressure at the downstream instrumentation module. In addition, the inlet and exit static pressures were independently measured using static pressure taps located at the center of each side of the instrumentation modules.

5.3.2.2. Coolant Side. The inlet and outlet coolant temperatures were measured using copper-constant thermocouples. Thermocouples mounted in stainless steel tubing were positioned at the centerline of piping elbows just before entering the top tank and immediately after leaving the bottom tank.

Coolant flow rate was measured using a Brooks rotameter calibrated by weighed discharge as a function of time. Atmospheric pressure was obtained using a mercury barometer.

5.4. Results and Discussion:

The computer program was used in designing the optimum heat pipe heat exchanger for a design heat duty of 10,000 Btu/hr. The design parameters such as the diameter, length and operating temperature, of heat pipes along with the exchanger variable including the transverse and longitudinal pitch are obtained as part of the optimization process. The heat exchanger was fabricated according to the optimized variables. The heat exchanger was tested for maximum heat transfer capacity and tested for performance against a range of variables. These are as follows:

- Air velocity from 300 - 3100 fpm

- Coolant flow rate 2 to 10 gpm
- Heat pipe damage simulation 0,2, and 5 heat pipes
- Heat pipe orientation.

The air flow around the pipes and its velocity control the heat transfer coefficient, and hence the heat rejected by the heat pipes to the environment. This is also true in the case of coolant, only that in this case, higher flow rates induce an increased heat transfer from the coolant to the heat pipes. Also, one should remember that superior thermal characteristics of coolant warrants a much smaller surface area and velocity to transfer loads.

The battlefield damage to a tactical radiator is quite unpredictable. With that in view, all experiments were repeated for 1) a full complement of pipes, 2) with two pipes damaged, and 3) five pipes damaged. This represents more than 20% of the total pipes installed in the model exchanger.

The damage was simulated by replacing specific pipes with aluminum rods. Even though, under real conditions, the pipes may be cut, still they offer resistance to air. The ballistics were assumed to come from the side, although shrapnel from exploding shells could cause random damage.

In anticipation of possible installation problems, some heat pipes may have to be installed with the evaporator section over that of the condenser. The performance of the pipes, and by extension, the model heat exchanger, will be quite different. To analyze this situation, experiments were conducted by rotating the heat exchanger upside down. The data were taken over the complete range of air flow/coolant flow rates. In addition, the exchanger, in this orientation, was performance tested for vulnerability due to damage.

Wherever applicable, the experimental data are plotted together with the analytical curve, in order to facilitate easy comparison.

Figures 5-10 and 5-11 show the performance curves of the model heat exchanger as a function of air velocity. As we would expect, the increasing heat transfer coefficient contributes to a higher capacity up to a velocity of 2500 fpm before leveling off. The agreement between the experimental data and the computer generated curve shows the correctness of the computer program developed for model

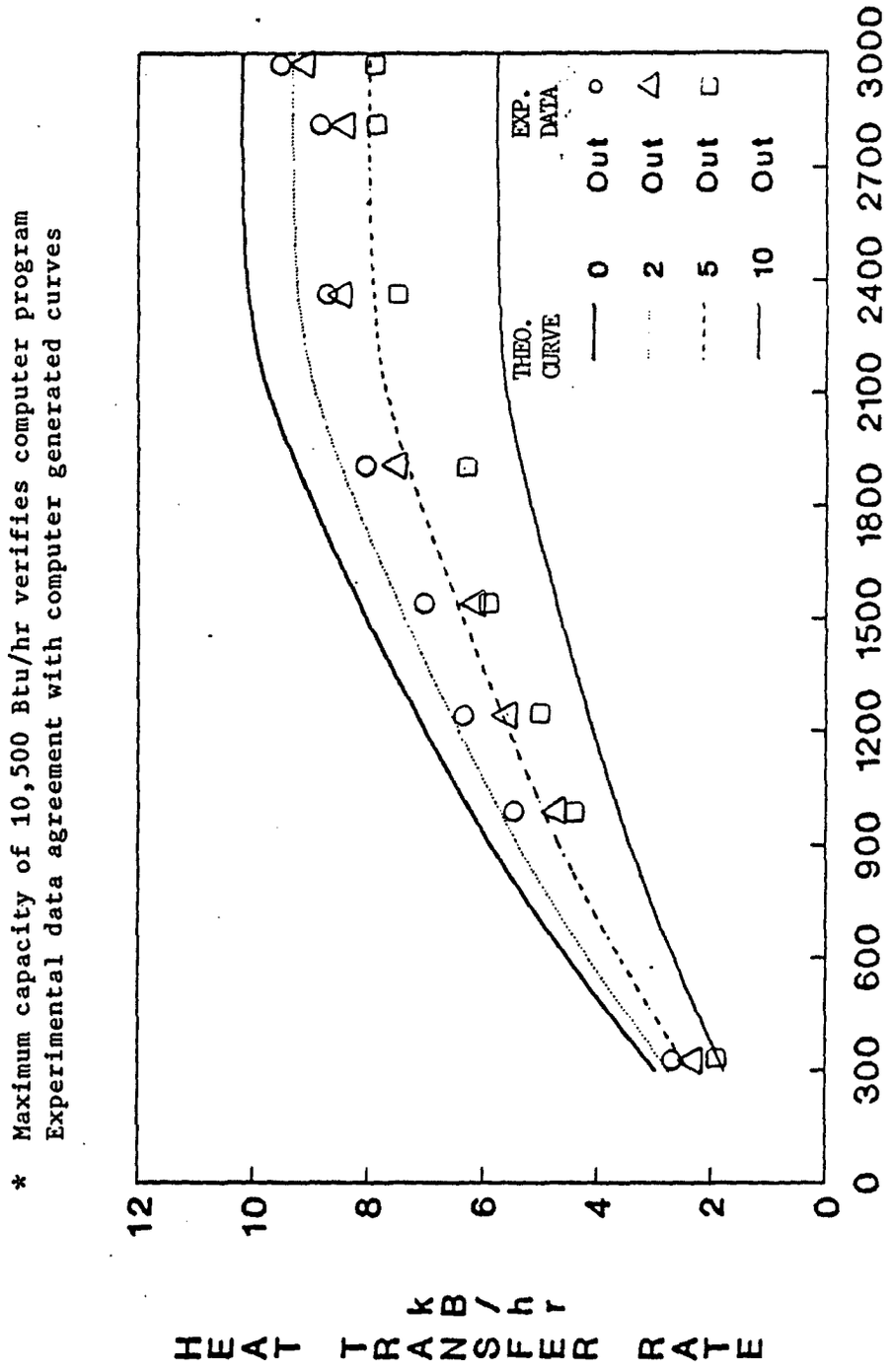

FIG. 8

Figure 5-10. Effect of Damage on Heat Pipe Network Water Flow - 10 gpm

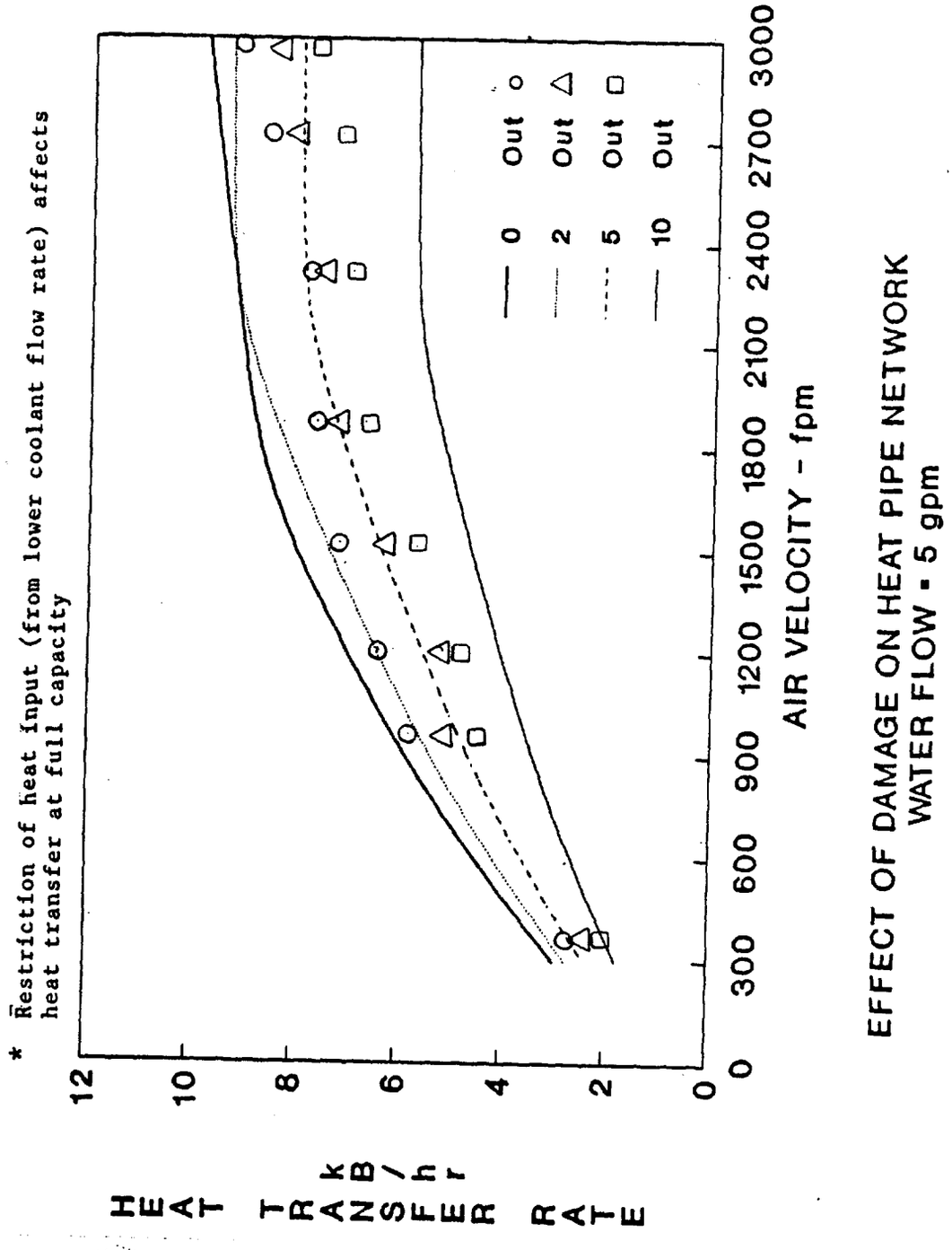

Figure 5-11. Effect of Damage on Heat Pipe Network Water Flow - 5 gpm

design. The curves for damage simulations, too, agree excellently with estimated values. At 10 GPM (see Figure 5-10) the evaporator section was able to absorb the rated load and the pipes were operating at near capacity. The removal of pipes do not impede the performance greatly. For instance, with 5 out of 23 pipes damaged, the performance reduction was around 15%. The curves for 40 % of the damaged pipes indicate the exchanger can still operate at more than 50% of its rated capacity.

When the coolant flow rate is decreased to 5 GPM (see Figure 5-11), the heat capacity of the fluid is still large enough to deliver a thermal load of nearly 10,000 Btu. (Of course, the coolant outlet temperature varied correspondingly.) It is easy to note that the load delivered by heat pipe network module was still increasing even at 3000 fpm, indicating the apparent restriction posed by heat input by coolant.

The constraint posed by the heat input is clearly seen in Figures 5-12 through 5-14. The curves show the heat transfer rate as a function of coolant flow, this time with near constant heat rejection to air. The module reaches its rated capacity only for flow rate > 7 GPM. This explains the rising trend exhibited by Figure 5-11. The data agree with the trend shown by the theoretical curves. The slight scattering of the data at low GPM is not uncommon and can be attributed to fluctuations in flow. Another noticeable feature is the flow rate at which the heat transfer becomes independent, decreases as more and more pipes are removed. The operating capacity of the severely damaged exchanger module can be expected to operate at close to 60 % capacity, with even a reduced liquid flow rate of 4 GPM.

The thermal capacity of the module reduces when the rejection rate is fixed at a lower level at V_{air} = 1500 fpm (see Figure 5-13). The data fall below the computed curves; however, the difference is below the experimental error. The plot indicates a reduction in capacity of 20% when air velocity is reduced from 2800 to 1500 fpm. Further reduction in air velocity 950 fpm (see Figure 5-14) decreases the heat exchanger performance by another 25%. Also, higher liquid flow rates (greater than 5 GPM) do not contribute positively to the performance.

The tests on damage simulation were conducted intuitively for two specific cases. Continuous curves were drawn by modifying the program and the estimated plots were checked with the available data for the two cases. With liquid flow maintained at maximum rate, the various vulnerability curves show that the performance reduction is more gradual at lower air velocity than at higher airflow rates (see Figure 515).

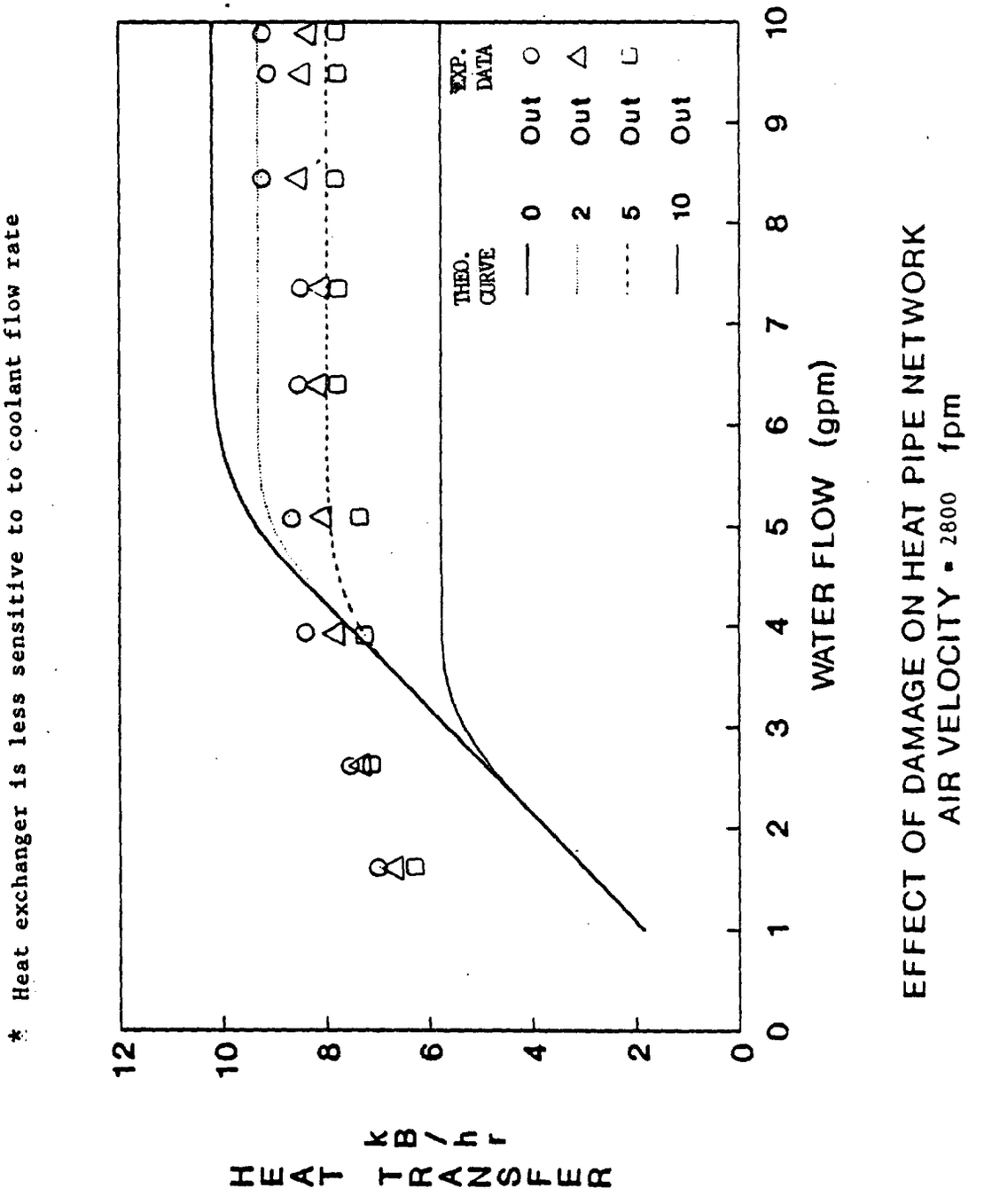

Figure 5-12. Effect of Damage on Heat Pipe Network Air Velocity - 2800 fpm

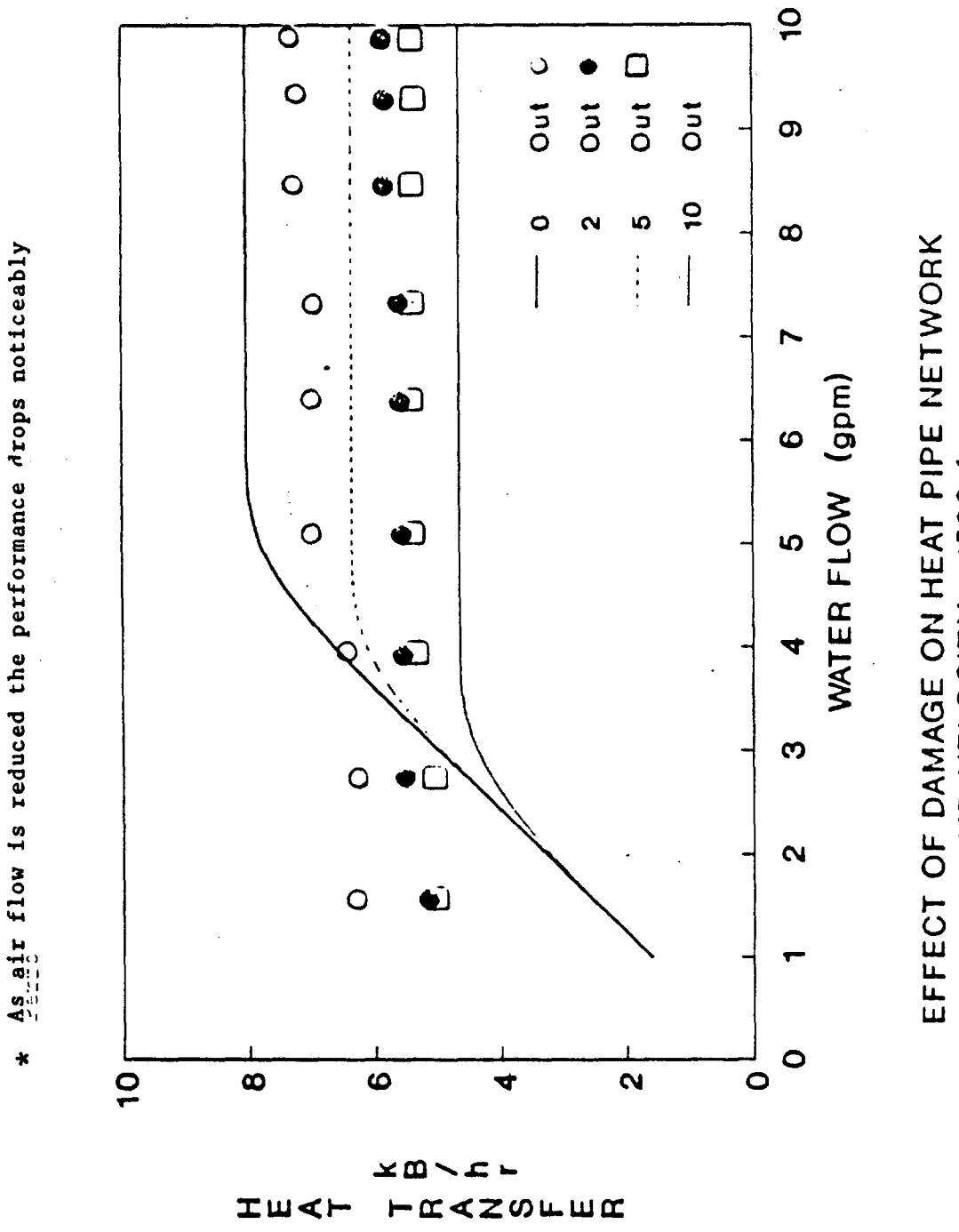

Figure 5-13. Effect of Damage on Heat Pipe Network Air Velocity - 1500 fpm

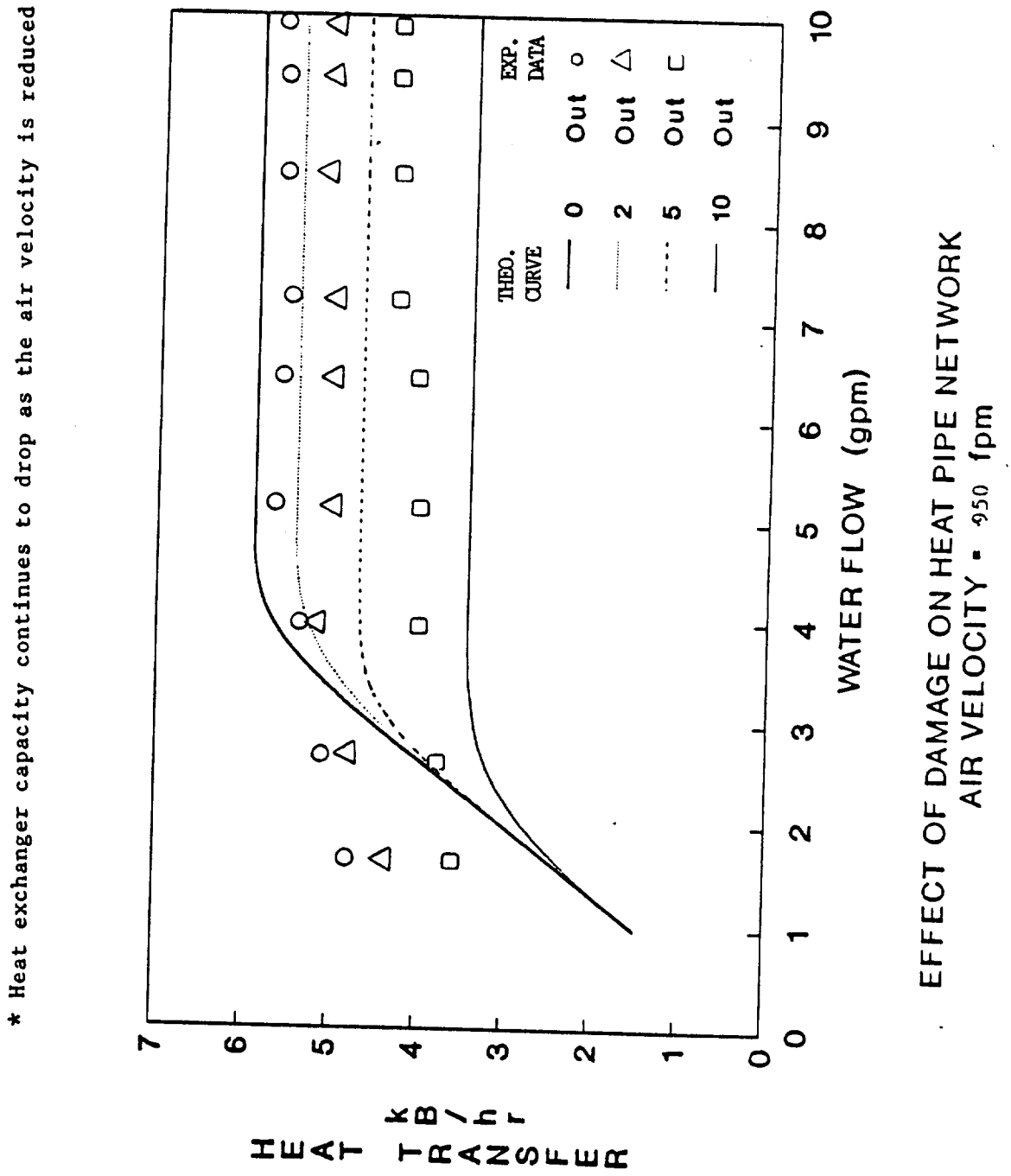

Figure 5-14. Effect of Damage on Heat Pipe Network Air Velocity - 950 fpm

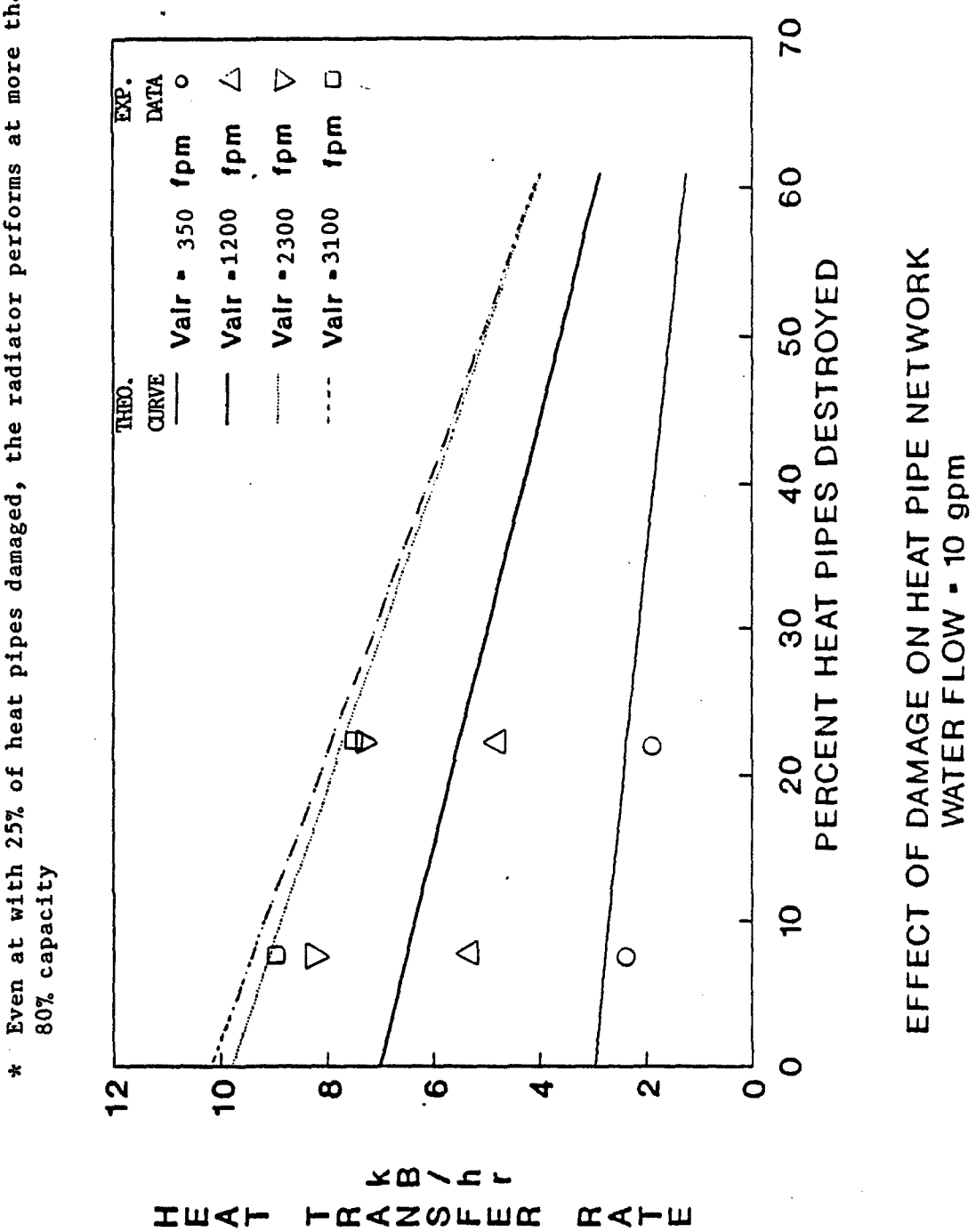

Figure 5-15. Effect of Damage on Heat Pipe Network Water Flow - 10 gpm

With sample data matching well with the curves, it is safe to say that the exchanger will continue to perform at 20 to 50% of its rated capacity with as much as 50% of the pipes destroyed depending on the air velocity.

Reduction in liquid flow rate on the module performance is noticeable for higher V_{air} of 2300 and 3100 fpm (see Figure 5-16). Comparing with the curves on Figure 5-15, it is clear that module operates somewhat less than 10,000 Btu/hr. But it maintains the performance at the same level with one or two pipes damaged.

Figures 5-17 and 5-18 show the same results in another form. Here we can observe that the combination of higher liquid and air flow rates, while transferring the rated capacity of heat, produces a drop that is steeper than at lower velocities.

A unique characteristic of any heat pipe network is that should some of the heat pipe ease to work, the remaining elements increase heat duty. This, however, is noticeable only if the heat pipes are operating under the maximum limit set by its elemental design. This can be seen in Figures 5-19 through 5-21. For example, in Figure 5-19, the pipes are already operating at near the upper limit (V_{air} = 3100 fpm, G = 5 to 10 GPM), the increase in individual heat pipe capacity is very small. But when heat exchanger is operating at lower (2.5 GPM) thermal loads, the heat transfer by a single pipe can increase as much as 70%. Caution should be exercised in that this value is still well below the upper limit set for the heat pipe. This characteristic is exhibited for any air velocity (see Figures 5-19 through 5-21).

Heat flux characteristics are shown as a function of the air velocity and increase in heat flux is minimal at high GPM and air velocities for reasons cited previously. Although heat fluxes are nearly the same, it should be pointed out that the net load decreases with damaged heat pipes (see Figures 5-22 and 5-23).

The heat pipe operation depends on the inside fluid circulation and this is sustained by capillary pumping and the gravitational force, which may aid or obstruct efficient operation. The data and the curves shown so far are gravity-assisted heat pipes.

When gravitational forces act against capillary forces, some of the pumping is lost and the heat pipe operates in an entirely different level.

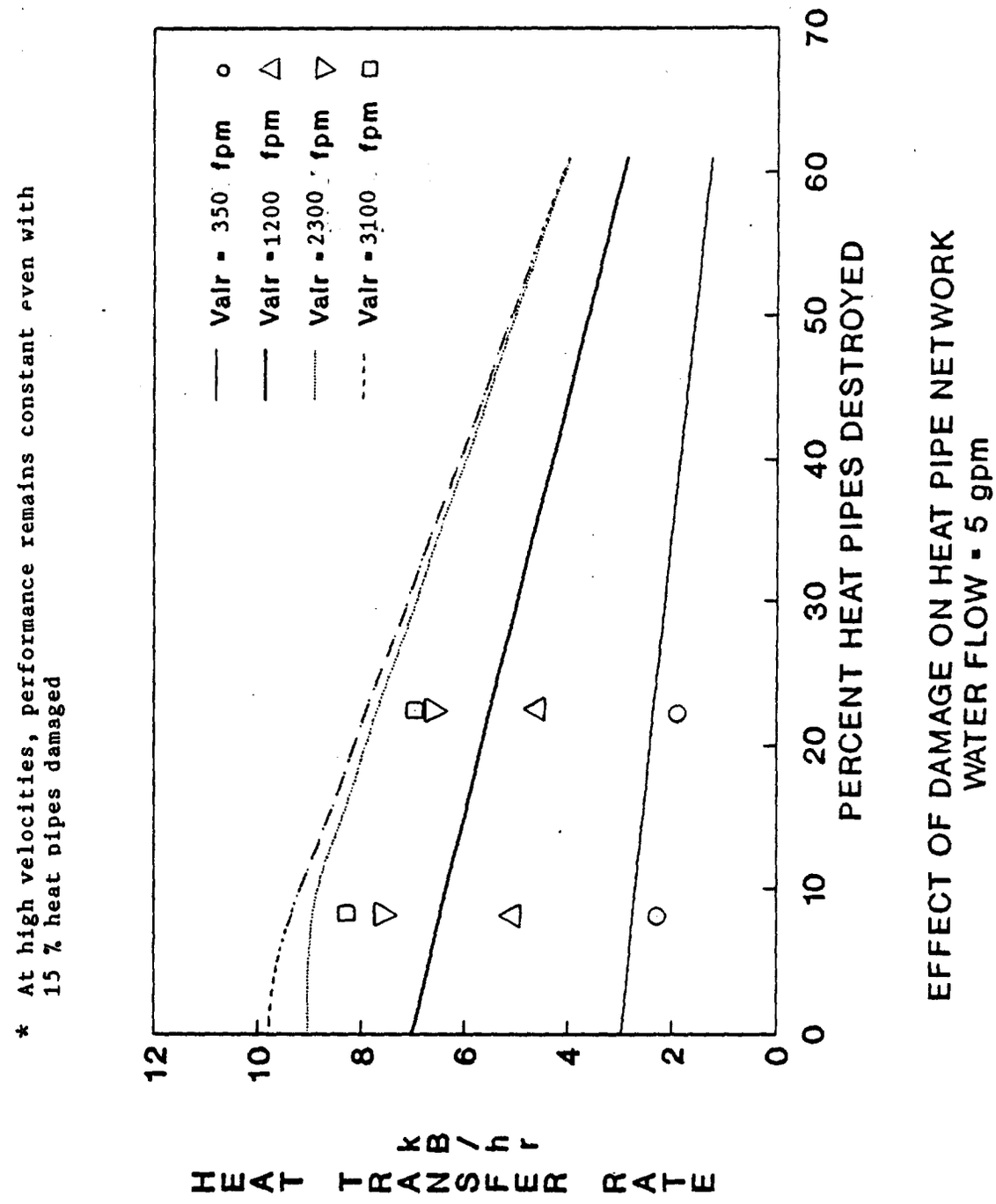

Figure 5-16. Effect of Damage on Heat Pipe Network
Water Flow - 5 gpm

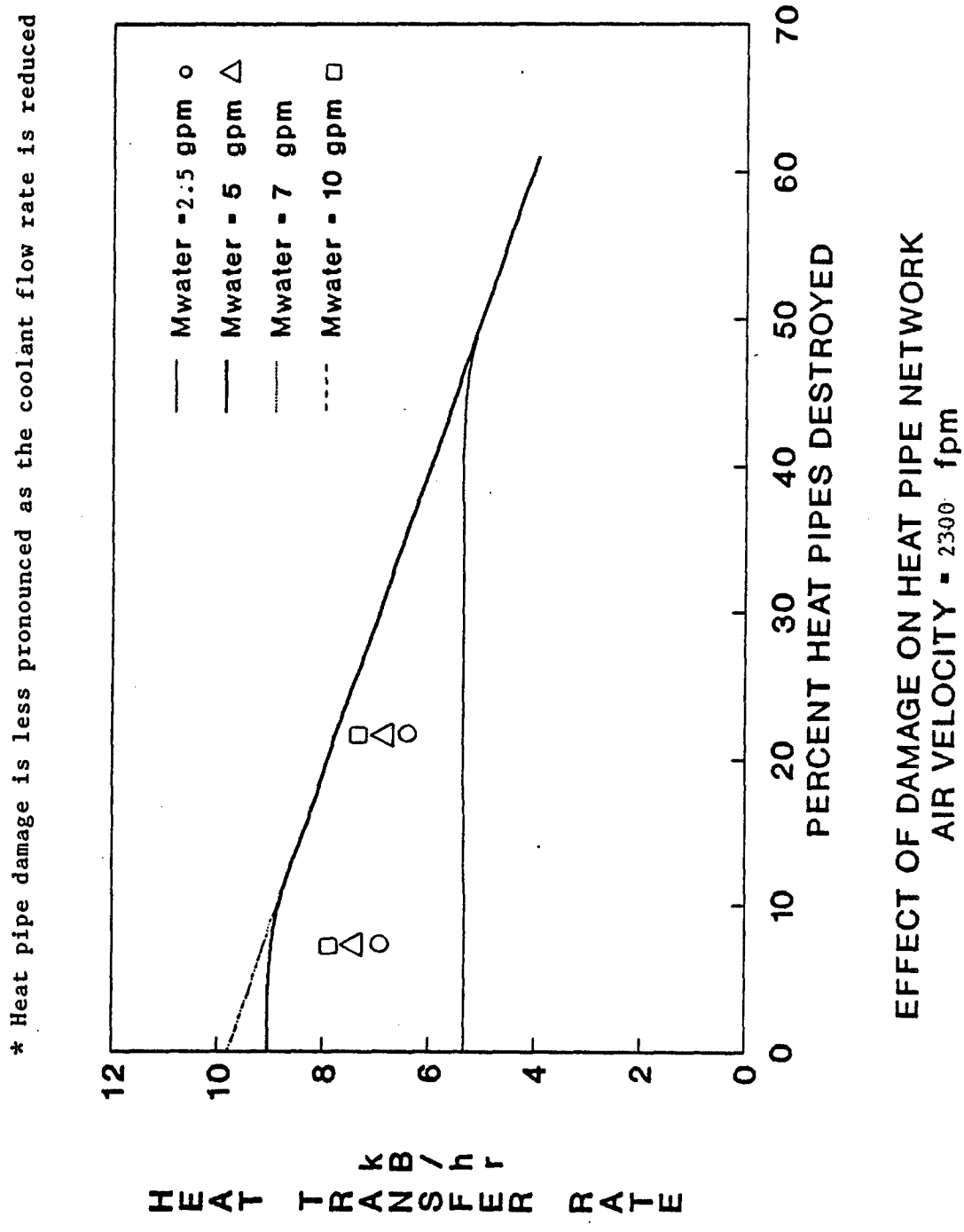

Figure 5-17. Effect of Damage on Heat Pipe Network Air Velocity - 2300 fpm

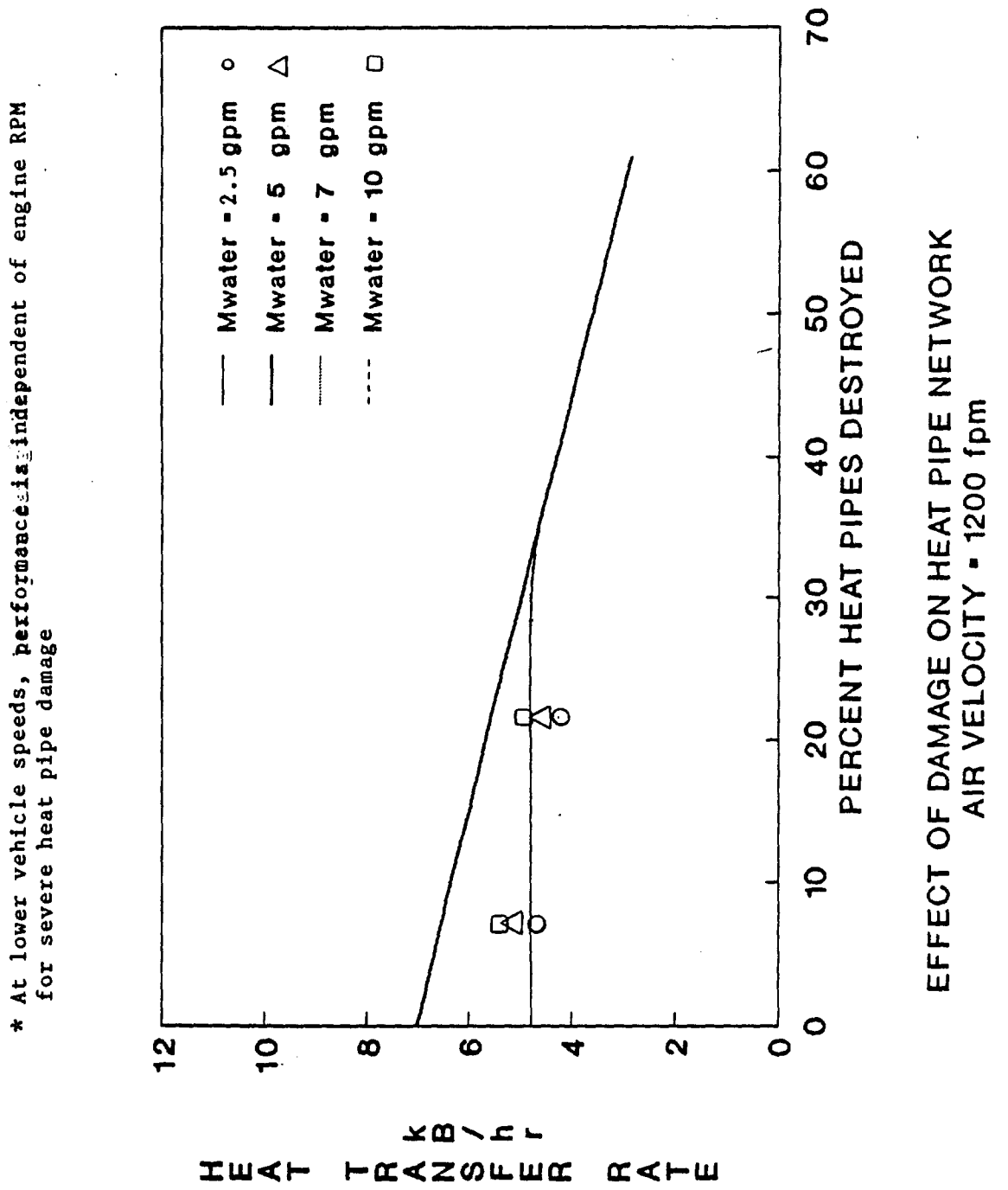

Figure 5-18. Effect of Damage on Heat Pipe Network Air Velocity - 1250 fpm

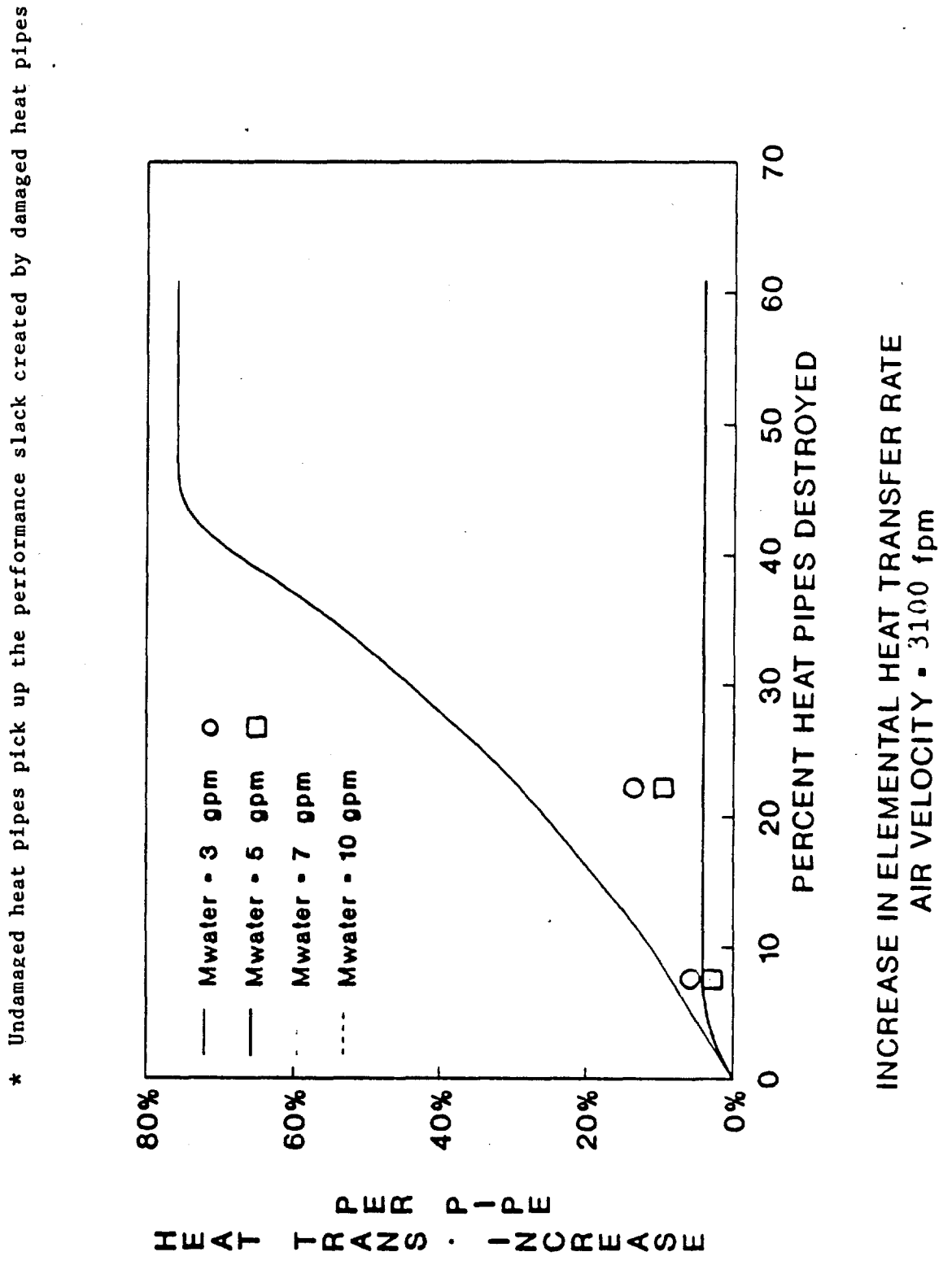

Figure 5-19. Increase in Elemental Heat Transfer Rate Air Velocity - 3100 fpm

* At lower air velocity, damage compensation becomes constant when 50% of the heat pipes are damaged

* Effect of air speed on

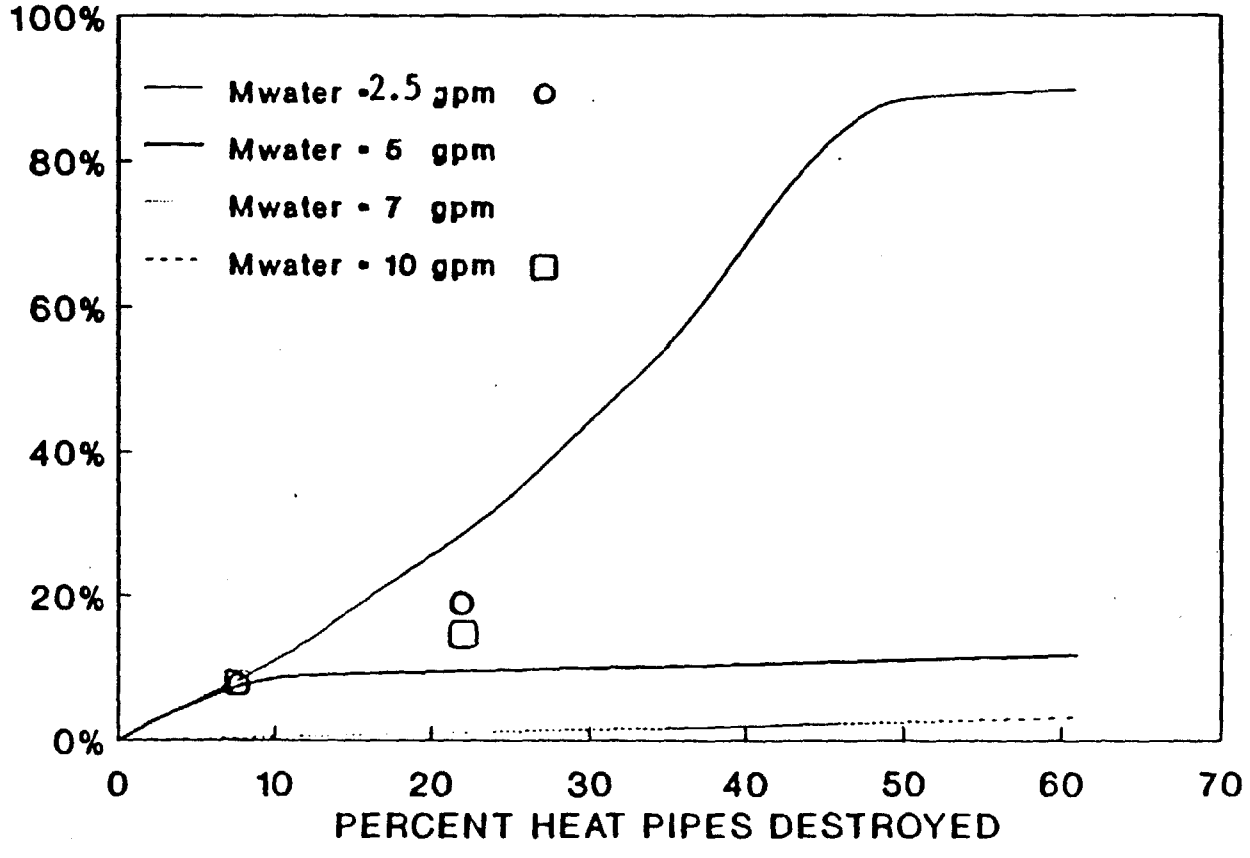

INCREASE IN ELEMENTAL HEAT TRANSFER RATE
AIR VELOCITY • 2300 fpm

Figure 5-20. Increase in Elemental Heat Transfer Rate Air Velocity - 2300 fpm

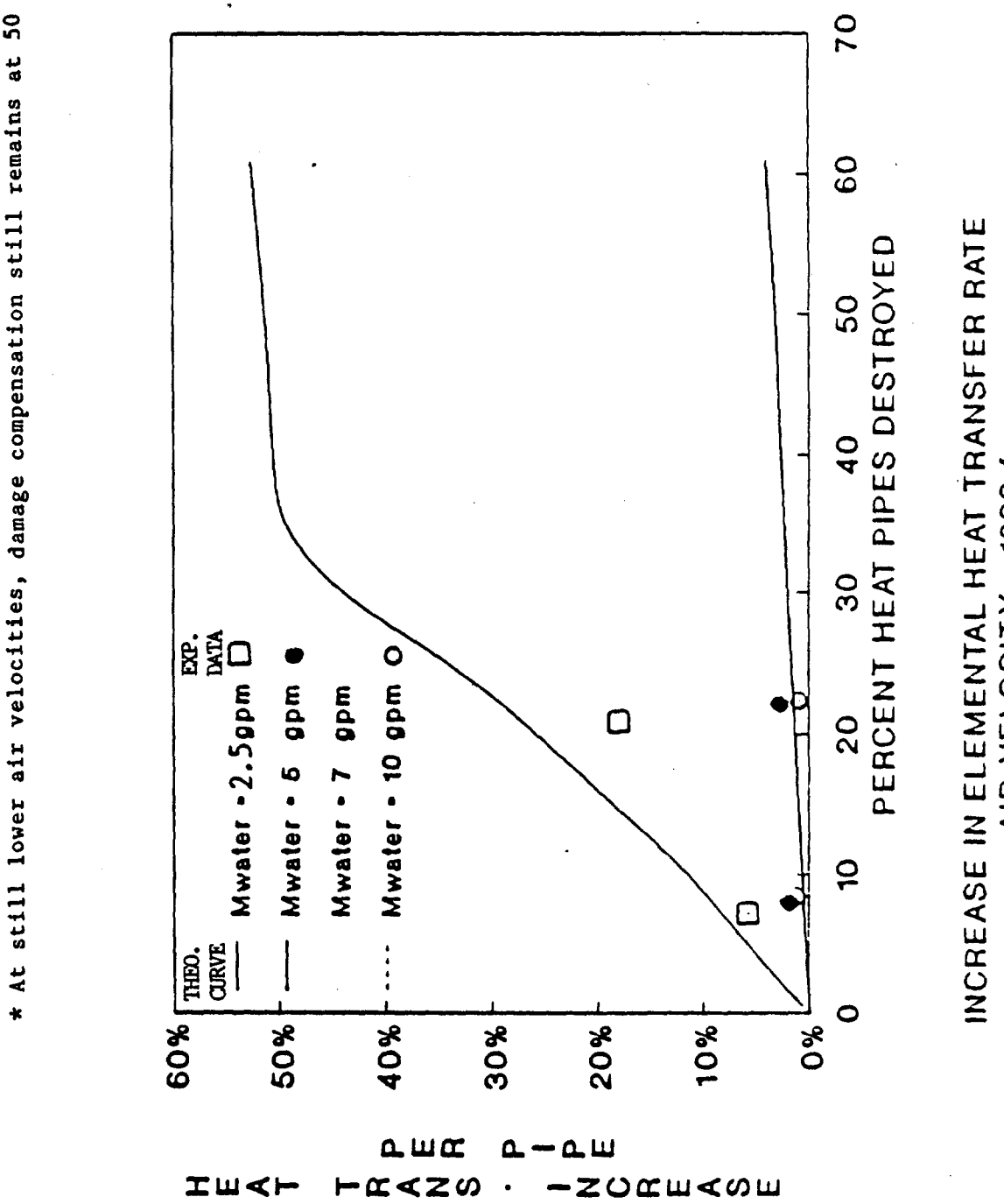

Figure 5-21. Increase in Elemental Heat Transfer Rate Air Velocity - 1200 fpm

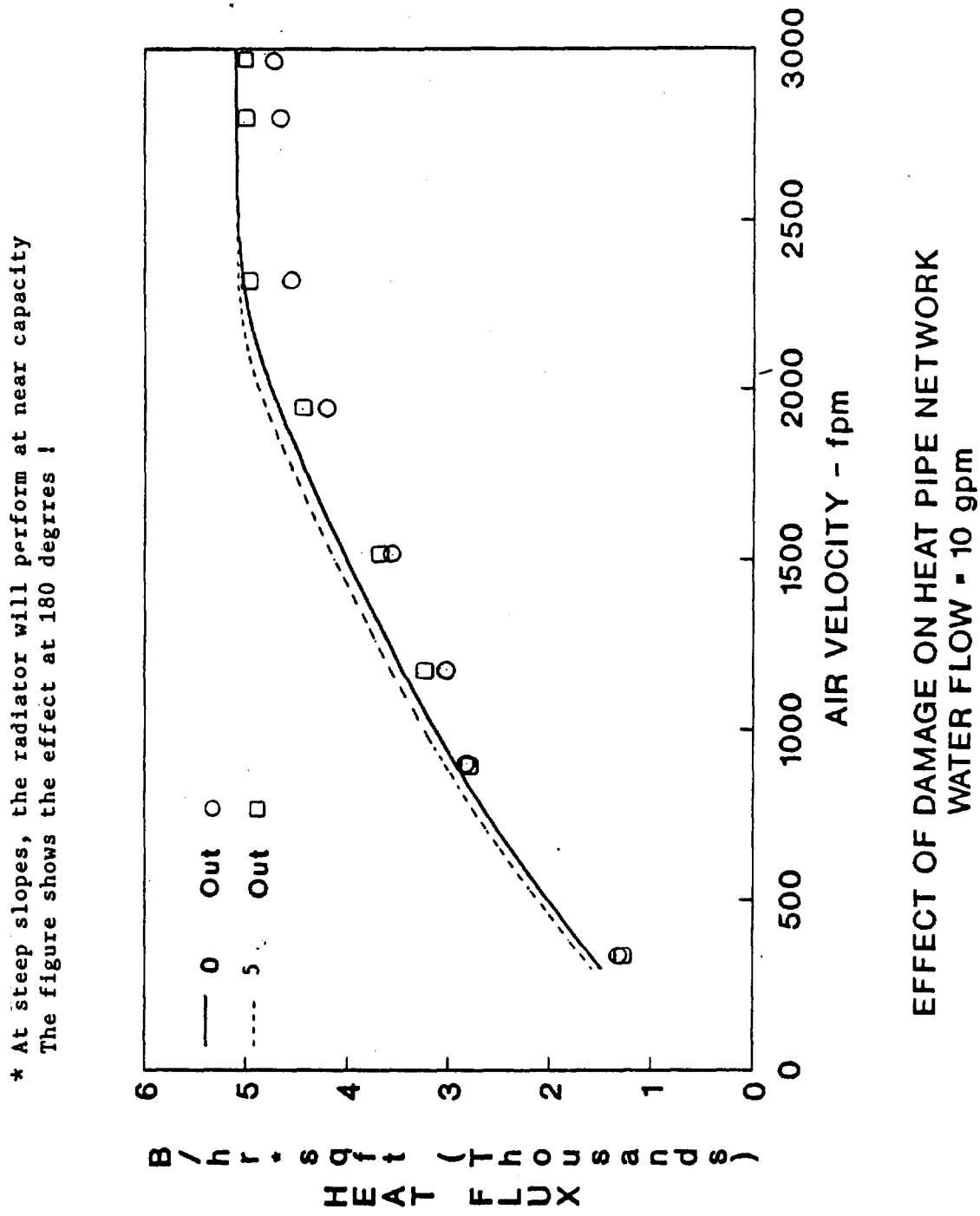

Figure 5-22. Effect of Damage on Heat Pipe Network Water Flow - 10 gpm

* A horizontal heat pipe radiator design should be avoided, if at all possible

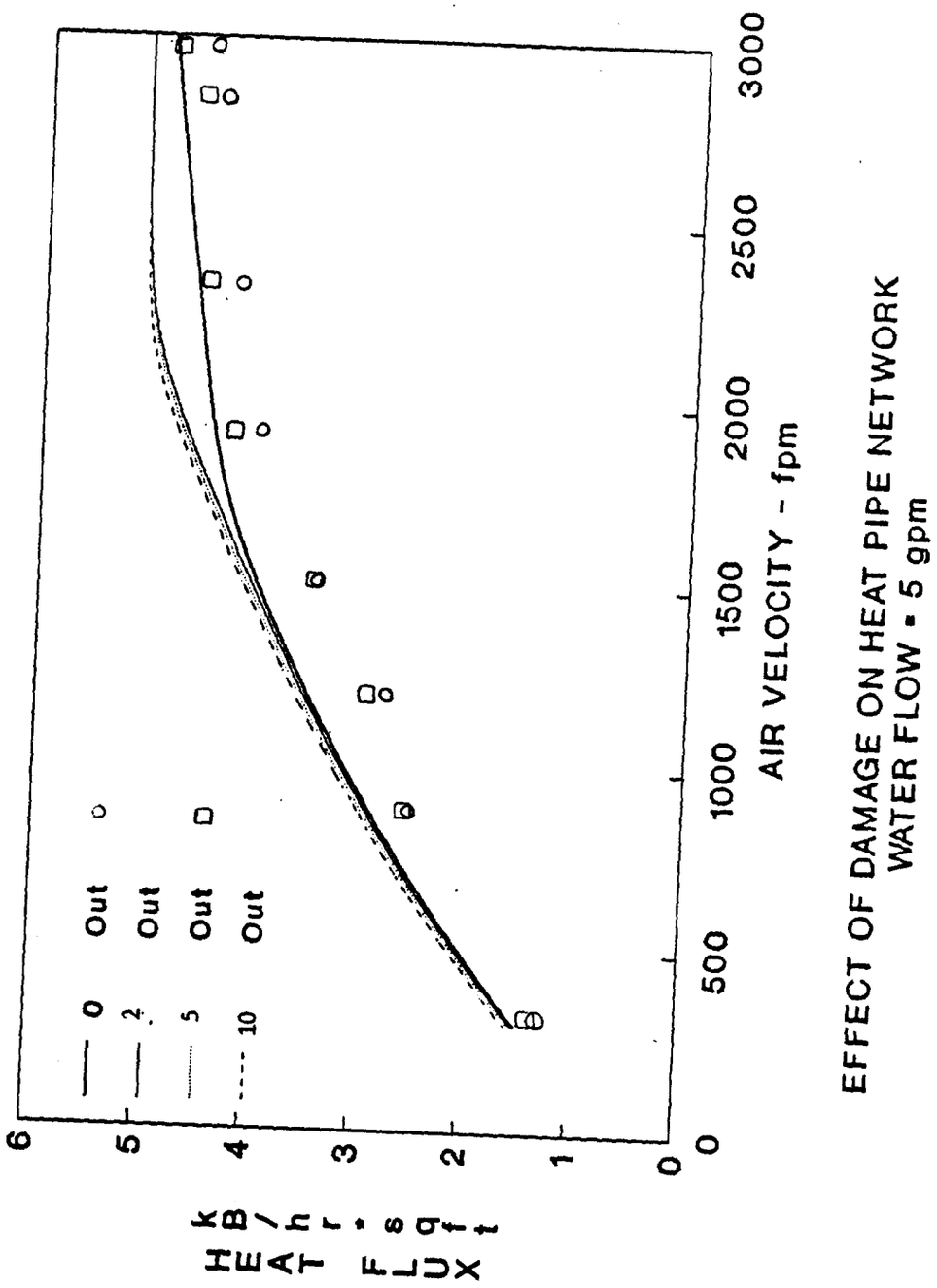

Figure 5-23. Effect of Damage on Heat Pipe Network Water Flow - 5 gpm

In Figure 5-24, a substantial reduction is shown in the overall capacity of the heat exchanger from 10,000 Btu/hr to 4,200 Btu/hr even at high air velocity (3,000 fpm) and coolant flow rates (10 GPM). The agreement of the experimental data with the theoretical estimates can be seen for both the full heat exchanger and with five pipes out. The behavior or the trend of the curves is quite similar to that exhibited in earlier curves that were drawn with gravity-assisted pumping.

A reduced heat input through a lower flow rate of 5 GPM results in almost identical curves (see Figure 5-25). It is because the heat pipes are working at maximum capacity even at flow rates less than 5 GPM. So any attempt to increase heat load through higher air or liquid flow rate will be futile. However, it must be pointed out that the only restriction is placed by the heat pipes since neither heat transfer coefficient nor the temperatures are affected by gravity.

Figure 5-26 shows the effect of airflow rates on pressure drop and heat transfer. The heat transfer characteristics were already explained previously (see Figure 5-10). The pressure drop behavior is as expected for a typical cross flow heat exchanger. The pressure drop increases exponentially with air velocity. We should recall that even with damaged heat pipes, the resistance to air flow remains the same.

The performance of the heat pipe heat exchanger module was compared with an equivalent conventional heat exchanger. The only difference between these two modules is the replacement of the heat pipes with the same diameter and the addition of a header at the top.

A proprietary cross flow heat exchanger program was used in the performance analysis of this heat exchanger and the results are compared with those of the heat pipe module (see Table 5-1).

As before, coolant and airflow rates were varied. The heat transfer capability of the heat pipe module is higher by up to 25%. At higher air and coolant flow rates, the difference is much greater. It may be expected that for a prototype radiator, the operating conditions notwithstanding, the performance will be even greater. This is because the coolant flow rates, as well as air flow rates result in higher Reynolds number and, by extension, heat transfer.

* Even at maximum coolant flow rate and air velocity, the performance is remains at 50%

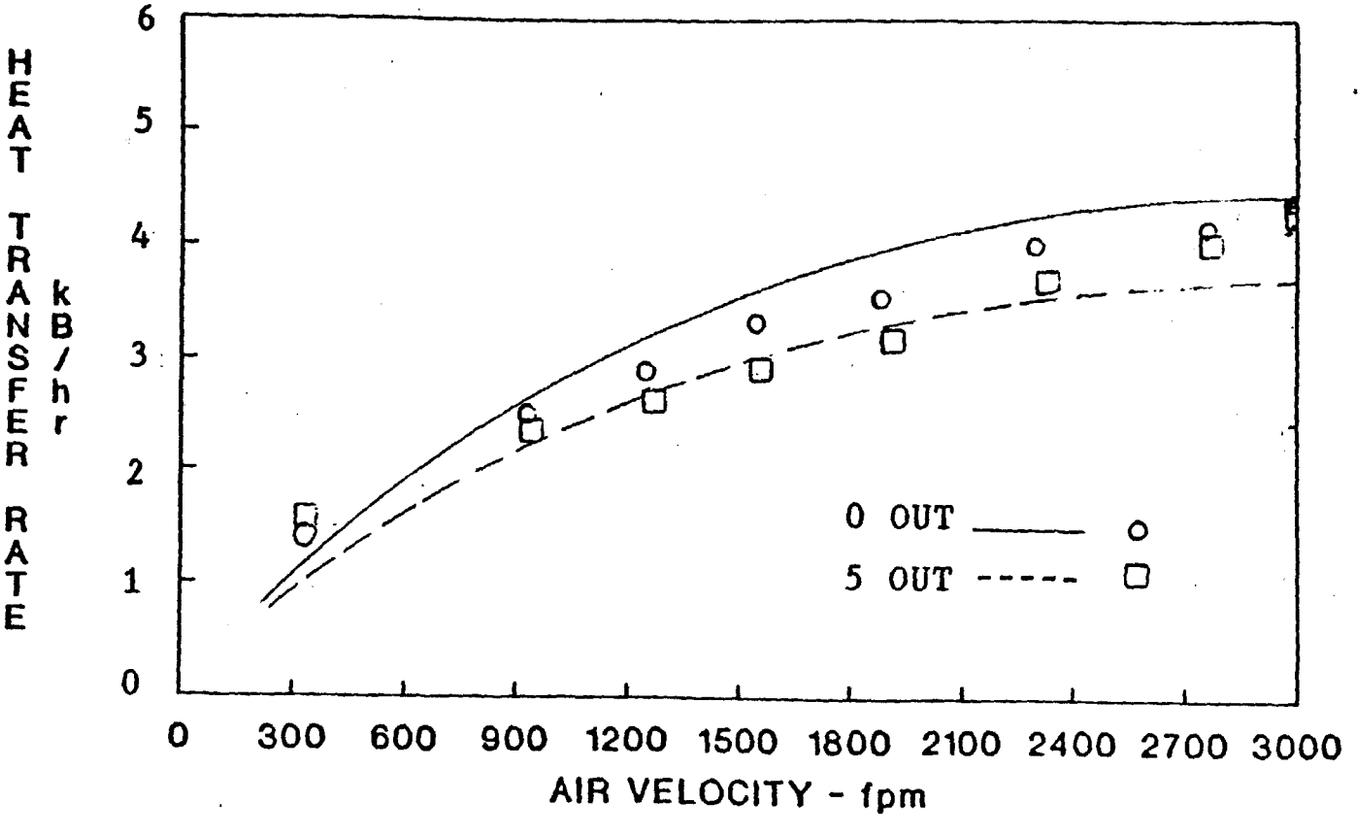

EFFECT OF DAMAGE ON HEAT PIPE NETWORK
WATER FLOW = 10 gpm
(AGAINST g)

Figure 5-24. Effect of Damage on Heat Pipe Network Water Flow - 10 gpm (against g)

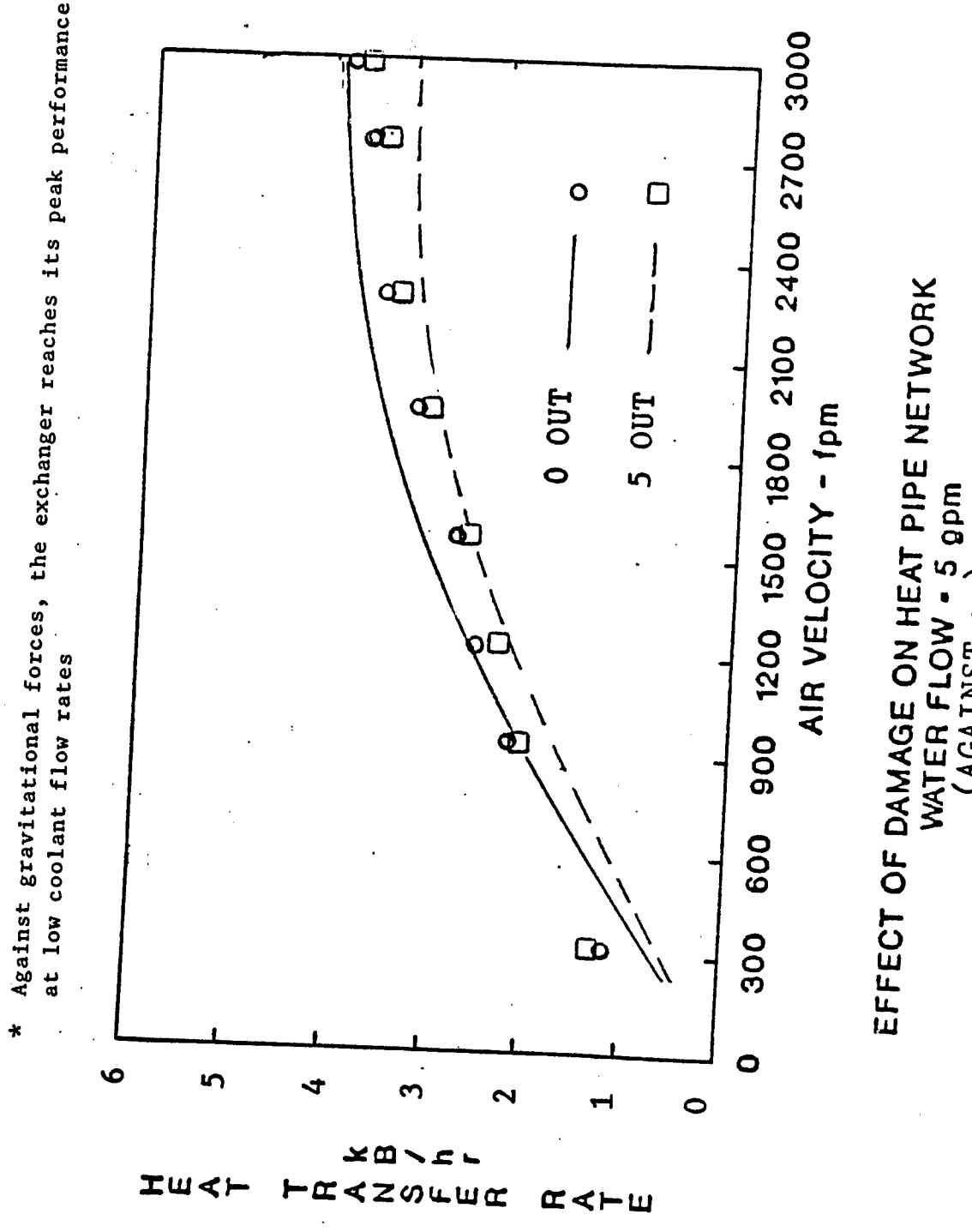

Figure 5-25. Effect of Damage on Heat Pipe Network Water Flow - 5 gpm (against g)

* Pressure drop trend is similar to that of a conventional Cross flow heat exchanger

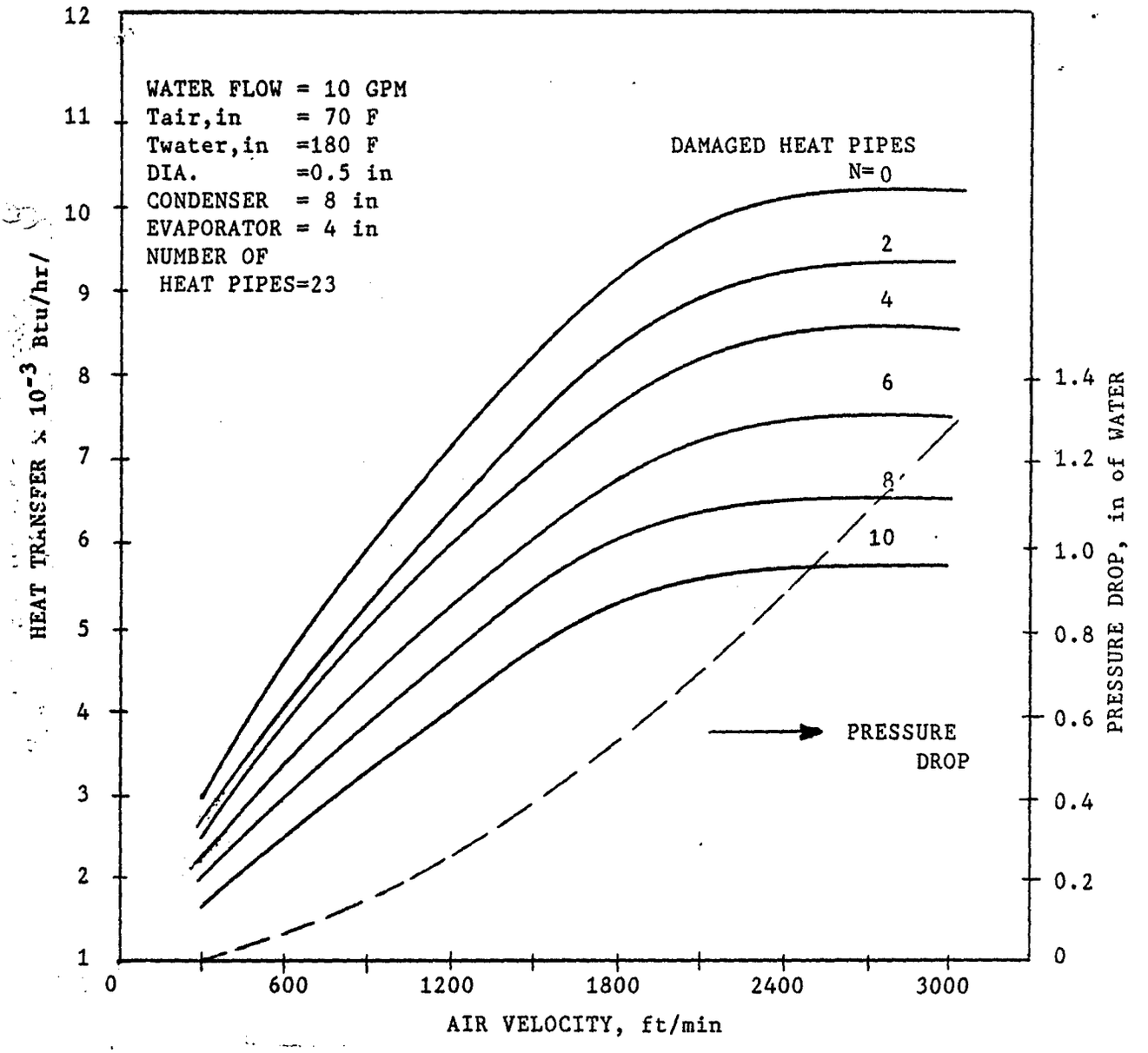

Figure 5-26. Effect of Air Velocity on Heat Transfer and P Pressure Drop

TABLE 1

Air Speed (fpm)	Water Flowrate (gpm) 10		5		3	
	Conventional Heat Exchanger Program (Btu/hr)	Heat Pipe	Conventional Heat Exchanger Program (Btu/hr)	Heat Pipe	Conventional Heat Exchanger Program (Btu/hr)	Heat Pipe
350	2025	1874	1967	2373	1938	2869
950	3613	3462	3534	4860	3416	5282
1200	4166	3987	4067	5271	3869	6123
1500	4712	4248	4588	6087	4340	6725
1950	5481	5393	5239	7152	4997	8041
2300	6084	5422	5704	7647	5419	8284
2800	6713	5422	6366	b7647	6018	8284
3100	7176	5422	6663	7647	6279	8284

Air inlet temperature $\simeq$ 75 - 84°F — For experiment

Air inlet temperature = 80°F — For conventional heat exchanger program

It may be stated with caution that a heat pipe radiator for similar loads can result in size and weight reduction.

The experimental data for the various tests are given in the Addendum.

5.5. Findings

- The experimental data are in excellent agreement with the theoretical curves, except at very low liquid and air flow rates which may be attributed to flow instabilities.
- Heat input effect is more pronounced; however, similar to air velocity influence, the performance becomes independent after certain critical liquid flow rates.
- The capacity of the module decreases with heat pipe, when the module is operating at high capacity.
- At lower thermal load, loss due to heat pipe, was compensated efficiently. With 30% of the pipes lost, the output from the remaining heat pipes increased by 40%. Yet, the individual heat pipe limit was still lower than the design upper limit.
- Against gravity, the flow rate did not have much liquid impact except at rates less than 5 GPM.
- The air flow rate increases the performance less gradually against gravity. Working against gravitational head, the decrease in thermal load was proportional to the percentage of damaged heat pipes.

In previous discussions it has been shown that the heat pipe consists of an evaporator section and the condenser section. For truck radiator applications, the evaporator section is placed in the hot coolant and the condenser section is swept by the air stream generated by the fan and the motion of the vehicle. The heat pipe is a self-contained closed system. These simple observations show that only one coolant header is required. The coolant will sweep the evaporator section and the air will receive the heat during flow over the condenser section.

By comparison, in the conventional radiator hot liquid enters the header at the top, flows through a bundle of tubes (downcomers) losing waste heat to cooler flowing air,

and is collected in a header at the bottom for return to the engine.

A conceptual heat pipe truck radiator could then be as shown in Figures 5-27 through 5-29. In this figure heat pipes are shown configured similarly to the coolant downcomers of a conventional radiator. A single coolant header is provided. This header could be armored or protected by the bumper of the vehicle. The radiator is then catastrophically vulnerable (capable of losing the entire engine coolant) only in the case of breakage of the main header or inlet/outlet hoses. Hits in other areas will only destroy certain heat pipe sections. It is seen that the area of vulnerability has been reduced significantly from the conventional radiator coolant tube configuration. Obviously, the entire engine coolant can be lost from a conventional radiator with a penetration in the top header, bottom header, and any coolant tube.

During Phase II, further testing will develop practical heat pipe configuration factors, such as length, shape, spacing, etc. A short condenser section requirement could significantly reduce the required length of the heat pipe. In this case, shorter heat pipes could be used. A potential configuration in this case could be as depicted in Figure 5-29. Two rows of half length heat pipes are shown using separate coolant headers. Each header could be armored against catastrophic failure.

More effective heat pipes could also reduce the size requirement (area) of the radiator, reducing vulnerability cross-sections. More advanced heat pipes using arterial wicks will lower the number of pipes required for similar conditions. Some possible alternative heat pipe designs that could be used are shown in Figure 5-30. Alternatively, by maintaining the same area as the conventional radiator more effective performance would be obtained and any pipes lost due to battle damage would result in less loss of cooling load. In this situation the radiator would be capable of sustaining a larger amount of battle damage. The tradeoffs necessary to make these judgements are complex and require the detailed data that would only be available during the Phase II effort.

This Phase I effort demonstrated the feasibility of the concept. Design parameters that are requred for tradeoff studies can only obtained from further testing and analysis. Operating conditions such as ambient air, less than $32^{o}F$ and greater than $120^{o}F$ should be taken into consideration. Heat pipe and radiator design, including consideration of alternative working fluids, will be taken into consideration

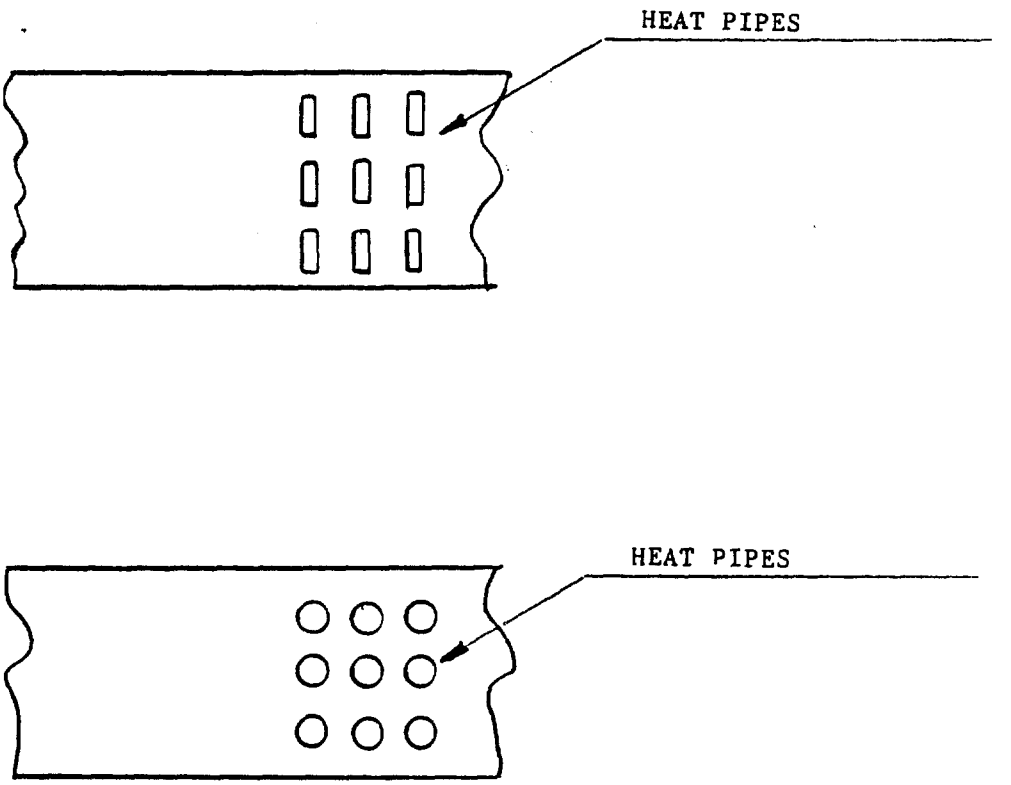

Figure 5-27. Possible Heat Pipe Arrangement

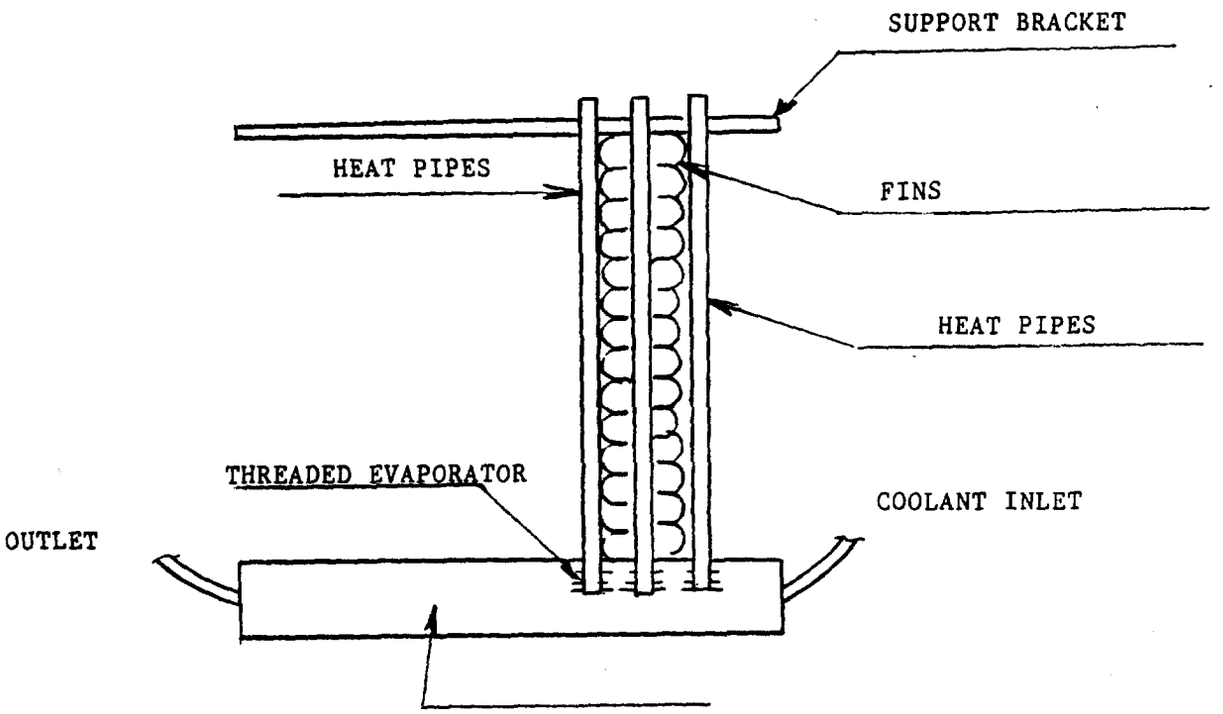

Figure 5-28. Single Window Heat Pipe Radiator Concept

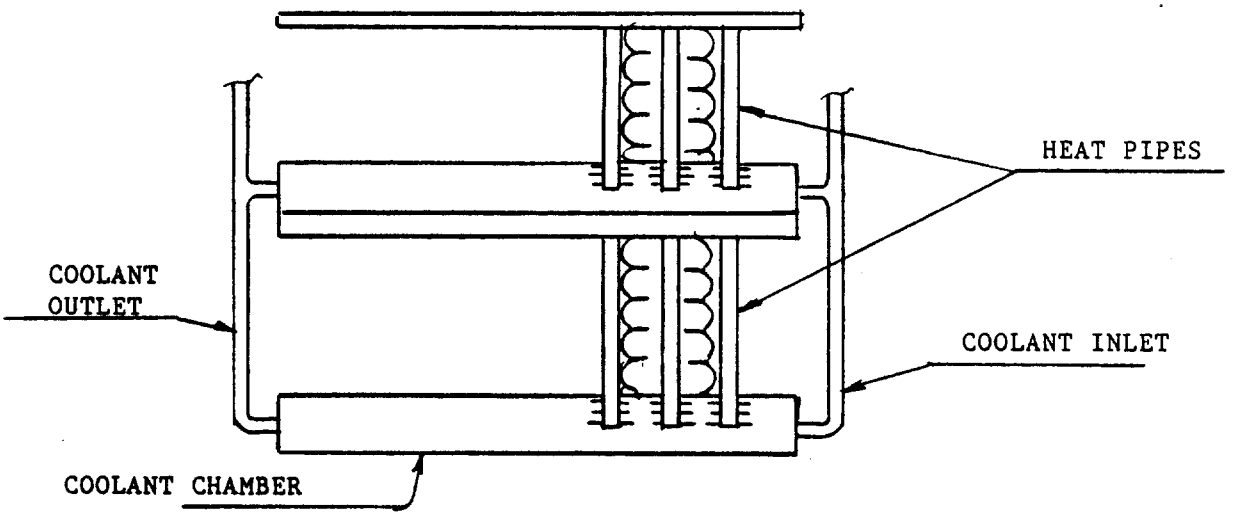

Figure 5-29. Dual Window Heat Pipe Radiator Concept

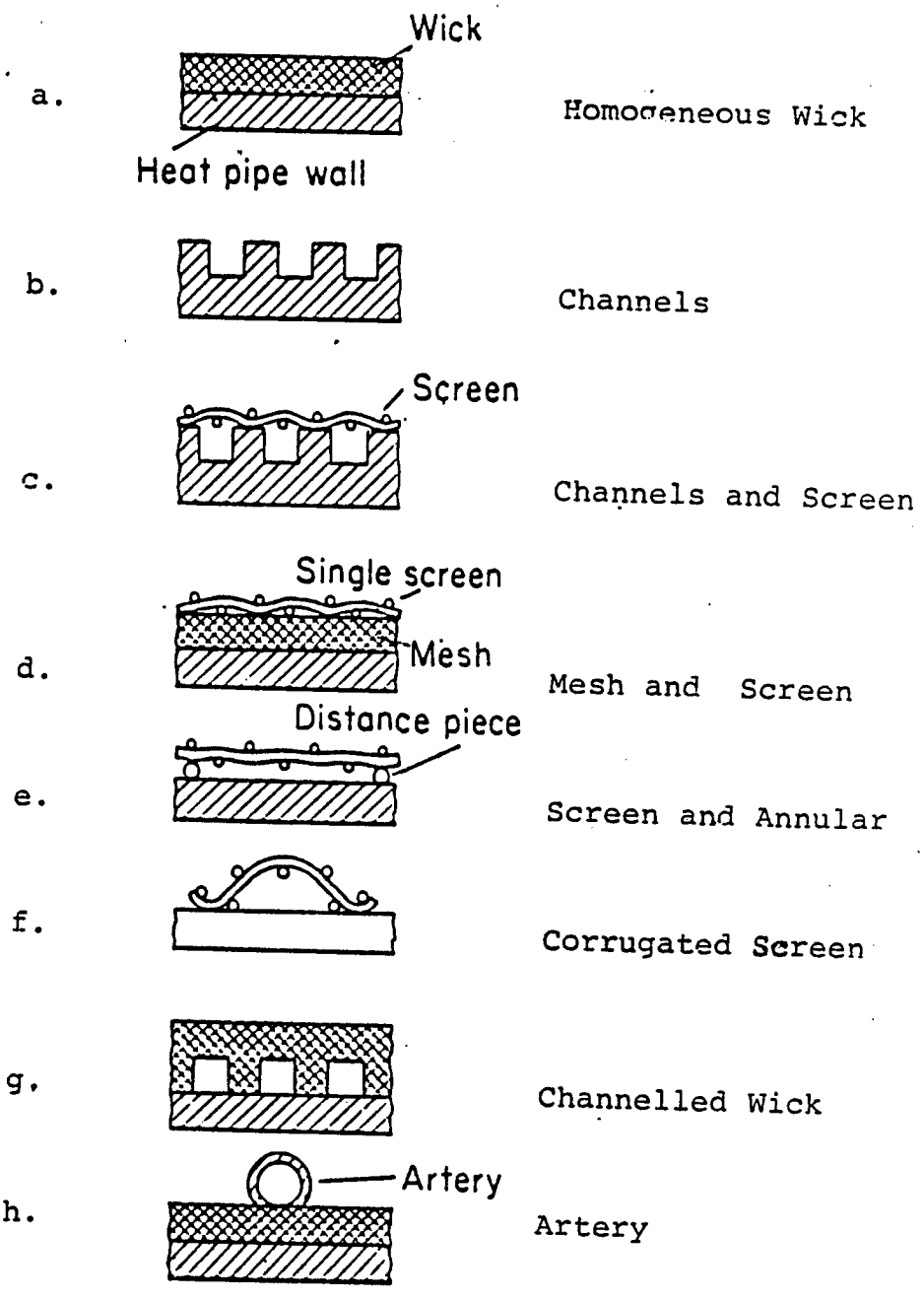

Figure 5-30. Geometric Arrangement of Wick Channels

in more detailed work beyond this "proof of concept" demonstration of a heat pipe network radiator.

This Phase I effort has demonstrated the feasibility of a heat pipe network to be used in application to a truck radiator. It has been shown that a heat pipe network can be accurately sized to meet a design cooling load at conditions approximating those of engine cooling. Furthermore, it has been shown that cooling load can be maintained with numerous pipes out of service such as could occur due to ballistic impact in a combat environment. By totally inverting the heat pipe matrix, it has also been shown that cooling load could be maintained at high slopes such as could be experienced in combat terrains.

Also, performance tests on the heat pipe network with water alone and 50/50 coolant glycol mixtures produced similar results that were within the experimental error.

Heat transfer capabilities of the heat pipe network have also been compared with those from a coolant system with geometry similar to the experimental configuration. The heat pipe network results in an effective 20 to 25% increase in heat transfer for the same geometry. This result shows the ability to lessen the area requirement for the radiator or to provide increased damage sustainability for the same area as the conventional coolant radiator.

This Phase I concept feasibility study has verified the thermodynamic capabilities of the net pipe network concept. Much more detailed analytical, experimental, and design studies are required before precise cost-benefit tradeoffs can be made as to adaptability to the Army requirements. A few observations can be made however, as a result of the studies conducted to date assuming that the final design approximates the conceptual study.

The chief modes of radiator failure, aside from ballistic projectile impact, are corrosion, fouling, and damage from foreign objects. The heat pipe radiator would have less surface exposed to the aerated corrosive cooling coolant. The only corrosion areas would be the external walls of the header and the surface area of contact between the hot coolant and the evaporator section of the heat pipe. The heat pipe itself is likely to be manufactured separately as an assembly and would use pure working fluids that would be corrosion proof to internal corrosion.

External fouling is due to dirt, mud, and engine oil dependent upon the manner in which the radiator installed in the engine compartment. Various configurations are possible

depending upon whether the compartment has positive or negative pressure. The test results to date have shown the heat pipe radiator to be potentially more efficient than the equivalent coolant radiator. With this potential available tube spacing could be opened up providing more air passage area. This could potentially reduce the tendency of external fouling.

The heat pipe radiator would also likely survive and continue to provide engine cooling even after damage to several tubes by rocks, branches, and other foreign objects. Conventional radiators would eventually lose all the cooling coolant even in the event of small penetrations in a tube or header.

Elimination of the other header (bottom header in the conventional radiator) would result in less cooling water total volume. This would also save coolant in combat but will also save glycol throughout the Army operational and training missions. Filling of the radiator and assuring no air pockets will be assured with the one header system and the closed cycle heat pipes. Conventional radiators at times lock the flow so that added coolant does not flow down to fill the downcomer tubes. In some instances, it is required to run the engine for a period then refill the radiator to insure complete filling.

With a proper design it is also possible that individual damaged heat pipes could be easily replaced. This would make field repairs much easier and could save on the need to stockpile entire radiator assembly for replacements.

Precise determinations on this matter will, of necessity, require a design close to the final one, such as will be attained in Phase II work. Conceptually, though, several possibilities could be postulated. The cost of the total radiator is likely to be controlled by the cost of the individual heat pipe elements. With volume production these costs would be significantly reduced from those used in the experimental test program. Taking advantage of the higher heat transfer ability of the heat pipes could also reduce the total number of elements necessary for incorporation into the radiator assembly, also reducing costs.

With the one header system, the number of braising operations could be reduced by about half compared with a conventional two header coolant downcomer radiator. The condenser ends of the heat pipes could be clamped in a support bracket and may not require braising.

It appears that, dependent upon the final design configuration that costs for the heat pipe radiator, in quantity could approximate those of the conventional radiator. Should the manufacturing costs be higher for the heat pipe radiator, it may be that when the combat operational benefits of the improved invulnerability are factored in that these costs could be justified.

LIST OF REFERENCES

1 AMCP 706-361, "Military Vehicle Electrical Systems," (in preparation)

2 MIL-C-45085B(AT), "Cooler, Oil, Transmission and Engine," (May 1968)

3 ATPD-2043, "Radiators, Engine Cooling, Military," (Purchase Description, Modification and Change to Military Specification is in progress) (October 1970)

4 TM750-254, "Cooling Systems: Tactical Vehicles," (March 1972)

5 "Cooling of Detroit Diesel Engines," General Motors Corp. Detroit Diesel Engine Division, Engineering Bulletin No. 28 (May 1967)

6 "Engineering Know-how in Engine Design - Part 15," SAE Publication SP-292 (1967)

7 Mascaretti, F.C. and Medana, R., "Diecasting Parts for Fiat Front Drive Cars," Proc. 7th SDCE Int. Diecasting Congress, Paper No. 4272 (1972)

8 Winship, J., "Diecasting Sharpens its Edge," American Machinist, Vol. 118, pp. 77-78 (1974)

9 Katzoft, S., "Heat Pipes and Vapor Chambers for Thermal Control of Spacecraft," AIAA Paper 67-310 (1967)

10 Roukis, J. et al., "Heat Pipe Applications for Space Vehicles, Grumman Aerospace," AIAA Paper 71-412 (1971)

11 Beard, R.A. and Smith, G.J., "A Method of Calculating the Heat Dissipation from Radiators to Cool Vehicle Engines," SAE paper 710208 (1971)

12 Cool, N.A., "Economic Factors in Radiator Selection," SAE paper 720714 (1972)

13 Tenkel, F.G., "Computer Simulation of Automotive Cooling Systems," SAE paper 740087 (1974)

14 Emmenthal, K.D. and Hucho, W.H., "A Rational Approach to Automotive Radiator Systems Design," SAE paper 740088 (1974)

15 SAE Handbook, Two volumes (1974)

16 Cotter, T.P., "Theory of Heat Pipes", USAEC Ref. LA-3246-MS, Contract W-7405-ENG-36, Los Alamos, NM; Los Alamos Scientific Laboratory, Univ. of Calif. (1965)

17 Busse, C.A., "Heat Pipe Research in Europe", 2nd Int. Conf. on Thermionic Electrical Power Generation, Stresa, Italy, May 27-31, 1968, Euratom Center for Information and Documentation (EUR No. 4210 f,e), pp. 461-475 (1969)

18 Busse, C.A., "Pressure Drop in the Vapour Phase of Long Heat Pipes", IEEE-Thermionic Conversion Specialist Conference, Palo Alto, CA, pp. 391-398 (October 30 - November 1, 1967)

19 Kinney, R.B. and Sparrow, E.M., "Turbulent Flow, Heat Transfer and Mass Transfer in a Tube with Surface Suction", J. Heat Transfer, pp. 117-125 (February 1970)

20 Silver, R.S. and Wallis, G.B., "A Simple Theory for Longitudinal Pressure Drop in the Presence of Lateral Condensation", Proc. Inst. Mech. Engrs., 180 (1), pp. 36-42 (1965/1966)

21 Brinkman, H.C., "On the Permeability of Media Consisting of Closely Packed Porous Interface", Appl. Sci. Res., Vol. A1, pp. 27-34 (1947)

22 Palen, J.W., "Heat Exchanger Sourcebook," Hemisphere Publishing Corporation, New York (1986)

23 Kays, W.M. and London, A.L., "Compact Heat Exchangers," 3rd Ed., McGraw-Hill, NY (1987)

24 Tubular Exchanger Manufacturers Assn. Standards, 5th ed. (1968)

25 Kern, D.Q., "Process Heat Transfer," McGraw, New York (1950)

26 Fraas, A.P. and Ozisik, M.N., "Heat Exchanger Design," Wiley, New York (1965)

27 Zhukanskas, A., "Heat Transfer from Tubes in Cross Flow", Advances in Heat Transfer, Vol. 8, NY (1972)

ADDENDUM

Air Flow: 1200 fpm N = 0

Coolant Flowrate (gpm)	Coolant		Air	
	in (°F)	out (°F)	in (°F)	out (°F)
10.0	180.9	179.6	77.7	87.9
9.4	182.0	180.6	77.1	87.8
8.3	180.9	179.2	77.1	88.0
7.1	182.0	180.1	76.5	87.2
6.3	182.6	180.5	75.9	86.4
5.0	182.6	180.1	75.9	86.1
3.8	182.6	179.1	75.9	86.4
2.5	180.9	176.6	75.9	84.3
1.5	182.6	175.6	75.7	84.1

Air Flow: 1500 fpm N = 0

Coolant Flowrate (gpm)	Coolant		Air	
	in (°F)	out (°F)	in (°F)	out (°F)
10.0	181.6	180.0	78.8	89.2
9.4	180.9	179.2	78.8	89.0
8.3	180.9	179.0	79.4	89.6
7.1	182.1	179.9	74.7	84.7
6.3	181.4	178.9	75.3	85.3
5.0	182.6	179.4	75.9	85.9
3.8	182.6	178.7	75.9	85.3
2.5	182.6	177.0	76.5	85.3
1.5	182.6	173.3	76.5	85.3

Air Flow: 1950 fpm N = 0

Coolant Flowrate (gpm)	Coolant		Air	
	in (°F)	out (°F)	in (°F)	out (°F)
10.0	180.9	179.1	80.6	89.3
9.4	182.0	180.2	81.8	90.2
8.3	180.3	178.2	81.8	90.2
7.1	182.6	180.1	81.2	89.9
6.3	182.0	179.3	81.2	89.4
5.0	177.5	174.1	80.6	88.8
3.8	178.6	174.5	80.0	87.6
2.5	180.6	174.4	79.4	87.0
1.5	180.3	170.8	79.4	86.4

Air Flow: 2300 fpm N = 0

Coolant Flowrate (gpm)	Coolant		Air	
	in (°F)	out (°F)	in (°F)	out (°F)
10.0	177.0	175.1	77.6	85.3
9.4	177.2	175.3	77.6	85.0
8.3	177.5	175.3	77.6	85.1
7.1	177.5	174.7	77.6	84.9
6.3	177.5	174.7	77.0	84.3
5.0	177.5	174.1	77.0	84.1
3.8	177.5	173.0	77.0	84.1
2.5	176.3	167.0	77.6	84.1
1.5	172.3	162.1	77.6	83.9

Air Flow: 2800 fpm N = 0

Coolant Flowrate (gpm)	Coolant in (°F)	Coolant out (°F)	Air in (°F)	Air out (°F)
10.0	178.6	176.7	78.2	84.8
9.4	177.5	175.4	78.2	84.9
8.3	176.9	174.5	77.6	84.4
7.1	176.3	173.6	78.2	84.6
6.3	176.3	172.5	78.2	84.6
5.0	176.3	172.5	77.6	84.1
3.8	175.7	170.7	77.6	84.1
2.5	175.7	168.7	77.6	83.5
1.5	174.0	163.6	77.0	82.3

Air Flow: 3100 fpm N = 0

Coolant Flowrate (gpm)	Coolant in (°F)	Coolant out (°F)	Air in (°F)	Air out (°F)
10.0	180.3	178.2	81.8	88.3
9.4	180.5	178.3	82.3	88.8
8.3	180.9	178.4	83.2	89.4
7.1	180.9	178.1	82.9	89.0
6.3	181.4	178.2	83.5	89.7
5.0	181.4	177.4	83.5	89.6
3.8	181.5	176.3	83.5	89.6
2.5	179.7	172.2	83.5	89.3
1.5	179.2	167.8	83.5	88.8

Air Flow: 350 fpm N = 2

Coolant Flowrate (gpm)	Coolant in (°F)	Coolant out (°F)	Air in (°F)	Air out (°F)
10.0	179.2	178.7	76.5	90.5
9.4	179.7	179.1	75.9	89.9
8.3	178.6	178.0	75.9	89.4
7.1	179.2	178.5	75.9	89.9
6.3	178.6	177.8	75.9	89.9
5.0	179.2	178.2	76.5	90.0
3.8	178.6	177.3	76.2	89.4
2.5	179.2	177.2	75.9	89.4
1.5	178.0	174.9	76.5	88.9

Air Flow: 950 fpm N = 2

Coolant Flowrate (gpm)	Coolant in (°F)	Coolant out (°F)	Air in (°F)	Air out (°F)
10.0	180.3	179.3	77.7	88.0
9.4	179.2	178.0	75.9	86.8
8.3	179.2	177.8	75.6	86.8
7.1	179.2	177.7	75.3	86.2
6.3	179.7	178.0	74.7	85.6
5.0	178.6	176.4	74.1	86.0
3.8	179.2	176.2	73.0	84.4
2.5	178.0	173.6	73.0	83.9
1.5	177.5	170.6	73.0	83.3

Air Flow: 1200 fpm N = 2

Coolant Flowrate (gpm)	Coolant		Air	
	in (°F)	out (°F)	in (°F)	out (°F)
10.0	179.2	178.0	78.8	88.2
9.4	179.2	177.9	78.8	88.2
8.3	179.7	178.3	78.8	88.2
7.1	180.3	178.7	79.0	88.2
6.3	179.2	177.4	78.8	87.8
5.0	179.2	176.9	78.8	88.0
3.8	179.7	176.8	78.6	87.4
2.5	178.6	174.5	78.2	86.8
1.5	178.6	171.7	78.2	86.4

Air Flow: 1500 fpm N = 2

Coolant Flowrate (gpm)	Coolant		Air	
	in (°F)	out (°F)	in (°F)	out (°F)
10.0	179.7	178.4	78.8	87.0
9.4	179.7	178.3	78.8	87.0
83.	178.6	177.0	78.2	86.4
7.1	179.2	177.5	78.8	86.6
6.3	179.2	177.2	78.2	86.0
5.0	180.3	177.8	78.2	86.0
3.8	178.6	175.4	78.2	86.0
2.5	179.2	174.3	77.0	84.8
1.5	179.2	171.6	77.0	84.2

Air Flow: 1950 fpm N = 2

Coolant Flowrate (gpm)	Coolant in (°F)	Coolant out (°F)	Air in (°F)	Air out (°F)
10.0	182.0	180.3	78.5	86.8
9.4	181.4	179.6	78.8	878.1
8.3	180.9	178.9	78.2	86.4
7.1	181.4	179.0	78.2	86.4
6.3	180.3	177.6	76.6	84.9
5.0	180.3	177.1	77.1	84.9
3.8	179.2	175.3	78.2	85.5
2.5	180.3	174.3	78.8	86.1
1.5	178.6	169.1	78.8	85.7

Air Flow: 2300 fpm N = 2

Coolant Flowrate (gpm)	Coolant in (°F)	Coolant out (°F)	Air in (°F)	Air out (°F)
10.0	179.7	177.9	73.5	81.0
9.4	179.2	177.3	73.5	80.9
8.3	179.7	177.5	74.7	82.1
7.1	179.7	177.2	73.5	80.9
6.3	180.3	177.5	73.5	80.8
5.0	180.3	177.0	74.1	80.9
3.8	179.7	175.3	75.3	82.1
2.5	179.2	173.0	74.7	81.0
1.5	177.5	167.2	74.1	80.4

Air Flow: 2800 fpm N = 2

Coolant Flowrate (gpm)	Coolant in (°F)	Coolant out (°F)	Air in (°F)	Air out (°F)
10.0	180.3	178.5	84.1	90.4
9.4	179.7	177.7	84.1	90.5
8.3	180.3	178.0	84.1	90.5
7.1	179.6	177.0	84.1	90.5
6.3	180.3	177.4	84.1	90.3
5.0	180.3	176.7	84.1	90.3
3.8	179.2	174.5	84.1	90.2
2.5	179.2	172.5	84.1	89.8
1.5	179.2	169.1	84.1	89.3

Air Flow: 3100 fpm N = 2

Coolant Flowrate (gpm)	Coolant in (°F)	Coolant out (°F)	Air in (°F)	Air out (°F)
10.0	180.3	178.2	80.6	87.0
9.4	180.3	178.1	81.8	88.2
8.3	180.3	177.8	81.8	88.2
7.1	180.3	177.6	82.3	88.2
6.3	180.9	177.9	82.3	88.2
5.0	179.7	175.9	82.3	88.1
3.8	180.3	175.3	82.3	88.2
2.5	179.7	172.4	82.9	88.5
1.5	178.6	167.1	82.3	87.6

Air Flow: 350 fpm N = 5

Coolant Flowrate (gpm)	Coolant in (°F)	Coolant out (°F)	Air in (°F)	Air out (°F)
10.0	180.3	179.9	78.8	91.1
9.4	181.4	180.9	78.4	90.5
8.3	180.3	179.7	78.2	90.5
7.1	180.9	180.3	78.2	90.5
6.3	180.9	180.2	78.2	90.2
5.0	181.4	180.5	78.2	90.3
3.8	180.3	179.2	78.8	90.5
2.5	180.9	179.2	78.8	90.5
1.5	180.9	178.2	79.4	90.5

Air Flow: 950 fpm N = 5

Coolant Flowrate (gpm)	Coolant in (°F)	Coolant out (°F)	Air in (°F)	Air out (°F)
10.0	180.3	179.4	75.3	84.7
9.4	180.3	179.3	74.7	84.1
8.3	180.9	179.8	75.3	84.7
7.1	180.9	179.6	75.3	84.7
6.3	180.3	178.8	76.2	85.3
5.0	180.3	178.5	76.5	85.6
3.8	180.9	178.6	77.1	85.9
2.5	179.7	176.3	77.1	85.6
1.5	179.7	174.2	77.1	85.3

Air Flow: 1200 fpm N = 5

Coolant Flowrate (gpm)	Coolant		Air	
	in (°F)	out (°F)	in (°F)	out (°F)
10.0	180.9	179.8	81.2	90.0
9.4	180.9	179.7	80.0	88.8
8.3	180.3	179.0	80.6	89.1
7.1	180.9	179.4	80.0	88.5
6.3	180.3	178.7	80.6	88.8
5.0	180.9	178.8	80.6	88.8
3.8	179.7	177.0	80.6	88.8
2.5	180.9	177.1	80.0	87.6
1.5	180.3	173.9	80.0	87.6

Air Flow: 1500 fpm N = 5

Coolant Flowrate (gpm)	Coolant		Air	
	in (°F)	out (°F)	in (°F)	out (°F)
10.0	179.7	178.5	81.2	88.8
9.4	180.9	179.6	81.2	88.8
8.3	179.7	178.3	80.6	88.2
7.1	180.3	178.6	80.6	88.2
6.3	180.3	178.4	80.0	87.6
5.0	179.7	177.3	80.0	87.6
3.8	180.3	177.2	79.4	87.0
2.5	180.9	176.5	80.0	87.0
1.5	179.2	171.9	80.6	87.6

Air Flow: 1950 fpm N = 5

Coolant Flowrate (gpm)	Coolant		Air	
	in (°F)	out (°F)	in (°F)	out (°F)
10.0	180.3	178.9	82.3	89.4
9.4	180.3	178.8	81.8	88.8
8.3	181.4	179.7	81.8	88.8
7.1	179.7	177.7	81.8	88.8
6.3	180.9	178.6	81.2	88.2
5.0	179.7	176.8	81.8	88.8
3.8	181.4	178.0	81.8	88.2
2.5	180.9	175.7	81.8	88.2
1.5	178.6	170.7	81.2	87.0

Air Flow: 2300 fpm N = 5

Coolant Flowrate (gpm)	Coolant		Air	
	in (°F)	out (°F)	in (°F)	out (°F)
10.0	180.3	178.6	81.8	88.8
9.4	180.9	179.1	81.8	88.8
8.3	179.7	177.7	81.8	88.8
7.1	180.9	178.5	81.8	88.8
6.3	180.3	177.6	81.2	88.2
5.0	179.7	176.6	81.8	88.2
3.8	180.3	176.2	81.2	87.6
2.5	180.9	175.1	81.2	87.2
1.5	178.6	170.2	81.2	86.4

Air Flow: 2800 fpm N = 5

Coolant Flowrate (gpm)	Coolant		Air	
	in (°F)	out (°F)	in (°F)	out (°F)
10.0	180.9	179.2	80.0	85.9
9.4	180.3	178.5	80.6	86.4
8.3	180.9	178.9	80.0	85.9
7.1	181.4	178.9	80.0	85.9
6.3	180.3	177.5	79.4	85.3
5.0	181.4	178.3	80.0	85.3
3.8	180.3	176.2	80.0	85.3
2.5	180.9	174.7	80.0	85.3
1.5	180.3	171.1	80.0	84.7

Air Flow: 3100 fpm N = 5

Coolant Flowrate (gpm)	Coolant		Air	
	in (°F)	out (°F)	in (°F)	out (°F)
10.0	180.3	178.6	80.0	85.3
9.4	181.4	189.6	81.2	86.4
8.3	181.4	179.4	81.2	86.4
7.1	180.3	177.9	80.6	85.9
6.3	180.9	178.3	81.2	86.4
5.0	181.2	177.8	81.2	86.4
3.8	180.3	175.9	81.2	86.4
2.5	180.9	174.4	81.2	86.2
1.5	179.2	169.7	81.2	85.6

Against g
Air Flow: 350 fpm N = 0

Coolant Flowrate (gpm)	Coolant in (°F)	Coolant out (°F)	Air in (°F)	Air out (°F)
10.0	179.2	178.9	81.2	88.8
5.0	179.7	179.2	81.8	88.8
2.5	187.6	177.9	81.8	87.6

Against g
Air Flow: 950 fpm N = 0

Coolant Flowrate (gpm)	Coolant in (°F)	Coolant out (°F)	Air in (°F)	Air out (°F)
10.0	179.7	179.1	80.6	86.2
5.0	178.6	177.5	80.0	85.3
2.5	178.0	176.4	80.6	85.3

Against g
Air Flow: 1200 fpm N = 0

Coolant Flowrate (gpm)	Coolant in (°F)	Coolant out (°F)	Air in (°F)	Air out (°F)
10.0	179.2	178.5	81.8	87.0
5.0	179.7	178.5	80.6	85.3
2.5	178.6	176.9	81.2	85.3

Against g
Air Flow: 1500 fpm N = 0

Coolant Flowrate (gpm)	Coolant in (°F)	Coolant out (°F)	Air in (°F)	Air out (°F)
10.0	178.6	177.9	81.8	86.4
5.0	179.2	177.9	81.8	85.9
2.5	179.2	177.4	81.8	85.3

Against g
Air Flow: 1900 fpm N = 0

Coolant Flowrate (gpm)	Coolant in (°F)	Coolant out (°F)	Air in (°F)	Air out (°F)
10.0	178.6	177.8	81.2	85.3
5.0	179.7	178.3	81.2	84.7
2.5	177.5	175.3	81.2	84.5

Against g
Air Flow: 2300 fpm N = 0

Coolant Flowrate (gpm)	Coolant in (°F)	Coolant out (°F)	Air in (°F)	Air out (°F)
10.0	179.2	178.3	80.8	84.5
5.0	179.2	177.6	80.1	83.5
2.5	178.6	176.3	80.0	82.9

Against g
Air Flow: 2800 fpm N = 0

Coolant Flowrate (gpm)	Coolant in (°F)	Coolant out (°F)	Air in (°F)	Air out (°F)
10.0	178.6	177.7	80.6	83.7
5.0	179.7	178.0	80.6	83.5
2,5	178.0	175.7	80.6	83.0

Against g
Air Flow: 3100 fpm N = 0

Coolant Flowrate (gpm)	Coolant in (°F)	Coolant out (°F)	Air in (°F)	Air out (°F)
10.0	179.2	178.3	80.6	83.5
5.0	179.2	177.5	80.6	83.2
2.5	178.6	176.1	80.6	82.9

Against g
Air Flow: 350 fpm N = 5

Coolant Flowrate (gpm)	Coolant in (°F)	Coolant out (°F)	Air in (°F)	Air out (°F)
10.0	180.3	179.9	81.8	90.5
5.0	180.3	179.7	81.5	89.4
2.5	179.2	178.3	81.8	88.8

Against g
Air Flow: 950 fpm N = 5

Coolant Flowrate (gpm)	Coolant in (°F)	Coolant out (°F)	Air in (°F)	Air out (°F)
10.0	180.3	179.8	79.4	84.7
5.0	179.2	178.3	80.6	85.3
2.5	178.0	176.6	80.6	84.7

Against g
Air Flow: 1200 fpm N = 5

Coolant Flowrate (gpm)	Coolant in (°F)	Coolant out (°F)	Air in (°F)	Air out (°F)
10.0	179.2	178.6	82.9	87.5
5.0	179.7	178.7	82.3	86.4
2.5	179.2	177.7	81.8	85.3

Against g
Air Flow: 1500 fpm N = 5

Coolant Flowrate (gpm)	Coolant in (°F)	Coolant out (°F)	Air in (°F)	Air out (°F)
10.0	179.2	178.5	80.6	84.7
5.0	179.7	178.6	82.3	85.9
2.5	178.6	177.0	82.3	85.3

Against g
Air Flow: 1950 fpm N = 5

Coolant Flowrate (gpm)	Coolant in (°F)	Coolant out (°F)	Air in (°F)	Air out (°F)
10.0	179.2	178.5	80.6	84.1
5.0	179.7	178.4	80.0	83.2
2.5	179.2	177.2	79.4	82.3

Against g
Air Flow: 2300 fpm N = 5

Coolant Flowrate (gpm)	Coolant in (°F)	Coolant out (°F)	Air in (°F)	Air out (°F)
10.0	179.7	178.9	81.2	84.7
5.0	179.2	177.8	80.6	83.5
2.5	178.6	176.3	80.6	83.4

Against g
Air Flow: 2800 fpm N = 5

Coolant Flowrate (gpm)	Coolant in (°F)	Coolant out (°F)	Air in (°F)	Air out (°F)
10.0	179.7	178.8	80.6	83.6
5.0	179.7	178.0	80.6	83.4
2.5	179.7	177.4	80.6	82.9

Against g
Air Flow: 3100 fpm N = 5

Coolant Flowrate (gpm)	Coolant in (°F)	Coolant out (°F)	Air in (°F)	Air out (°F)
10.09	178.6	177.6	80.6	83.5
5.0	179.2	177.5	80.6	83.2
2.5	178.6	176.3	80.6	82.7

LIST OF ABBREVIATIONS, ACRONYMS AND SYMBOLS

- A - surface area (ft^2)
- d - wick outside or surface diameter (ft)
- K - permeability (ft^{-2})
- l - length (ft)
- l_a - length of adiabatic section (ft)
- l_c - length of condenser (ft)
- l_e - length of evaporator (ft)
- l_{eff} - effective length (ft)
- m - mass flow rate (lbm/s)
- N - number of heat pipes
- ΔP - pressure drop (lb/ft^2)
- Q - heat rate (Btu/hr)
- q_e - entrainment limit (Btu/hr)
- R_e - Reynolds number (GD/μ) (-)
- r - wick inner radius (ft)
- r_c - pore size (ft)
- S_L - longitudinal pitch (ft)
- S_T - transverse pitch (ft)
- T - temperature (F)
- ΔT_{LMTD} - log mean temperature difference
- T_{in} - inlet temperature
- T_{out} - outlet temperature
- U - overall heat transfer coefficient ($Btu/hr/ft^2/F$)
- v - velocity (ft/s)

We - Weber number ($\rho v l / 2\pi\sigma_c$) (-)

Greek

ϵ - porosity, emissivity (-)

θ - angle of inclination (deg) (-)

λ - latent heat of vaporization (Btu/hr/lbm)

μ - dynamic viscosity (lbm/hr/ft^2)

ρ - density (lbm/ft^3)

σ_c - surface tension (lbf/ft)

Subscripts

a - air

c - capillary, condenser

e - evaporator, electrical

g - gravitation

i - inertial

l - liquid

s - sonic, surface

v - vapor

w - water

DISTRIBUTION LIST

	Copies
Commander Defense Technical Information Center Bldg. 5, Cameron Station Alexandria, VA 22304-9990	12
Manager Defense Logistics Studies Information Exchange ATTN: AMXMC-D Fort Lee, VA 23801-6044	2
Commander U.S. Army Tank-Automotive Command ATTN: ASQNC-TAC-DIT AMSTA-IRSA (Denise B. King) AMSTA-RGT (M.L. Goryca) AMSTA-CF (Mr. Orlicki) Warren, MI 48397-5000	 2 1 1 1
Commander U.S. Army Material System Analysis Activity (AMSAA) ATTN: AMXSY-MP (Mr. Cohen) Aberdeen Proving Ground, MD 21005-5071	1